Each item of HF data provided later in this document contains a small table identifying pertinent measurement and instrumentation parameters. These parameters are:

Line 1	Date in yymmdd format and local time
Line 2	Location, laboratory ID, measurement location
Line 3	Converter type, converter operational mode
Line 4	Center frequency, frequency span, IF frequency width, scan time
Line 5	Conductor, Probe ID, line amplifier gain, RF Attenuation, IF gain

The results presented in this report are obtained from a DC-to-DC converter employing solid-state switching techniques. The very short duration of the switching transients generates a wide noise spectrum whose amplitude cannot be defined by narrow-band measurements. In addition, the susceptibility of devices to the impulsive EMI is dependent on the bandwidth of each victim device (especially radio receivers). To resolve this problem, the measurements were made at a convenient bandwidth near the center of interest to most applications of the data, and a bandwidth conversion curve is used to adjust the data to the desired bandwidth. Figure 2.2-2 provides the bandwidth conversion curve. Hodges[4] developed this curve empirically from a large number of field measurements, and it permits noise measured at one bandwidth to be scaled to another bandwidth by adding or subtracting the appropriate value obtained from the curve. The value is expressed in dB, but it can be changed to a ratio for the extrapolation of data based on voltage or current measurements.

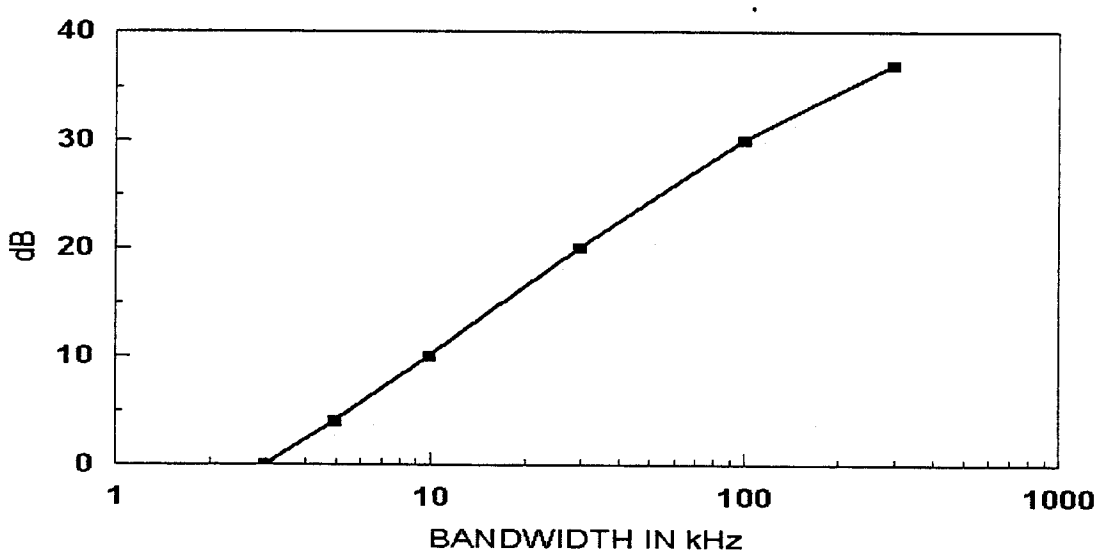

Figure 2.2-2

Bandwidth Correction Curve

[4] James W. Hodges, ***A Comparison between Power-Line Noise Level Field Measurements and Man-Made Radio Noise Prediction Curves in the High Frequency Radio Band***, MS Thesis, Naval Postgraduate School, Monterey, CA, December 1995

3. MEASURED RESULTS

3.1 Low-Frequency Results

Low-frequency results were obtained for two operating conditions. EMI current flowing on the 120-VAC input power conductors was measured with only the converter control circuits in operation and again with the inverter at full power. Additional measurements were made at intermediate power levels. This provided a means to compare EMI current flowing on the input power conductors for the two primary operating conditions.

Figure 3.1-1 shows the differential-mode current at 60 Hz and its low-order harmonics on the neutral (white) conductor of the power cord when only the control electronics was operating. The top view shows low-order harmonics up to 5 kHz. The bottom view shows an expanded view of the 60-Hz current and low-order harmonics up to 2 kHz.

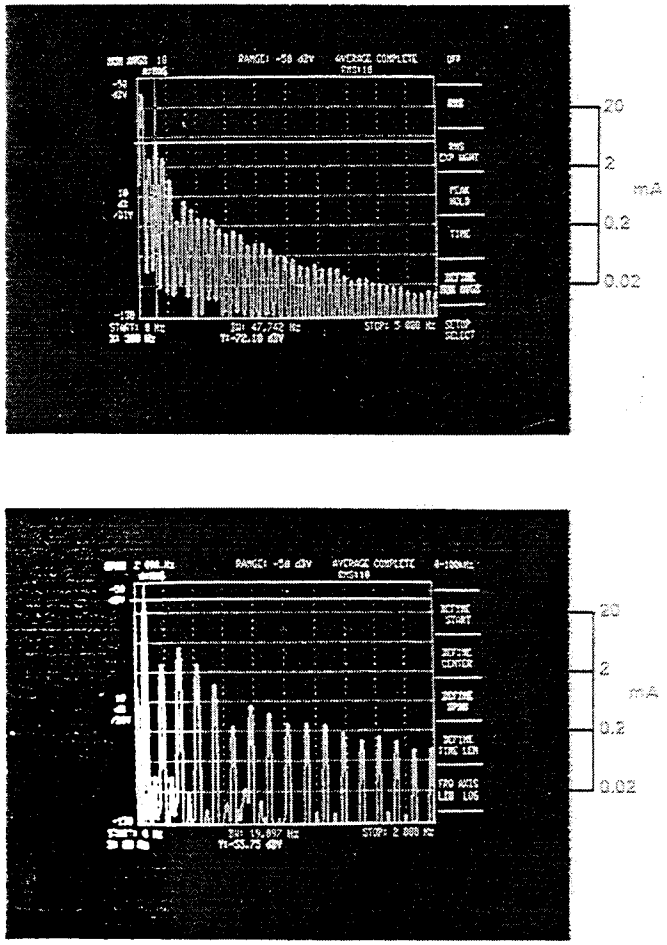

01 0501 1427

Figure 3.1-1

LF Current, White 120-VAC Conductor, Control Electronics Only

NPS, P2, 120V N
CONTROL PWR ONLY
W, CT4 (20/1), P6021 (10/1), +20

Figure 3.1-2 shows the differential-mode current at 60 Hz and its low-order harmonics on the hot (black) conductor of the 120-VAC power cord when only the control electronics was operating. The top view shows low-order harmonics up to 5 kHz. The bottom view shows an expanded view of the 60-Hz current and low-order harmonics up to 2 kHz.

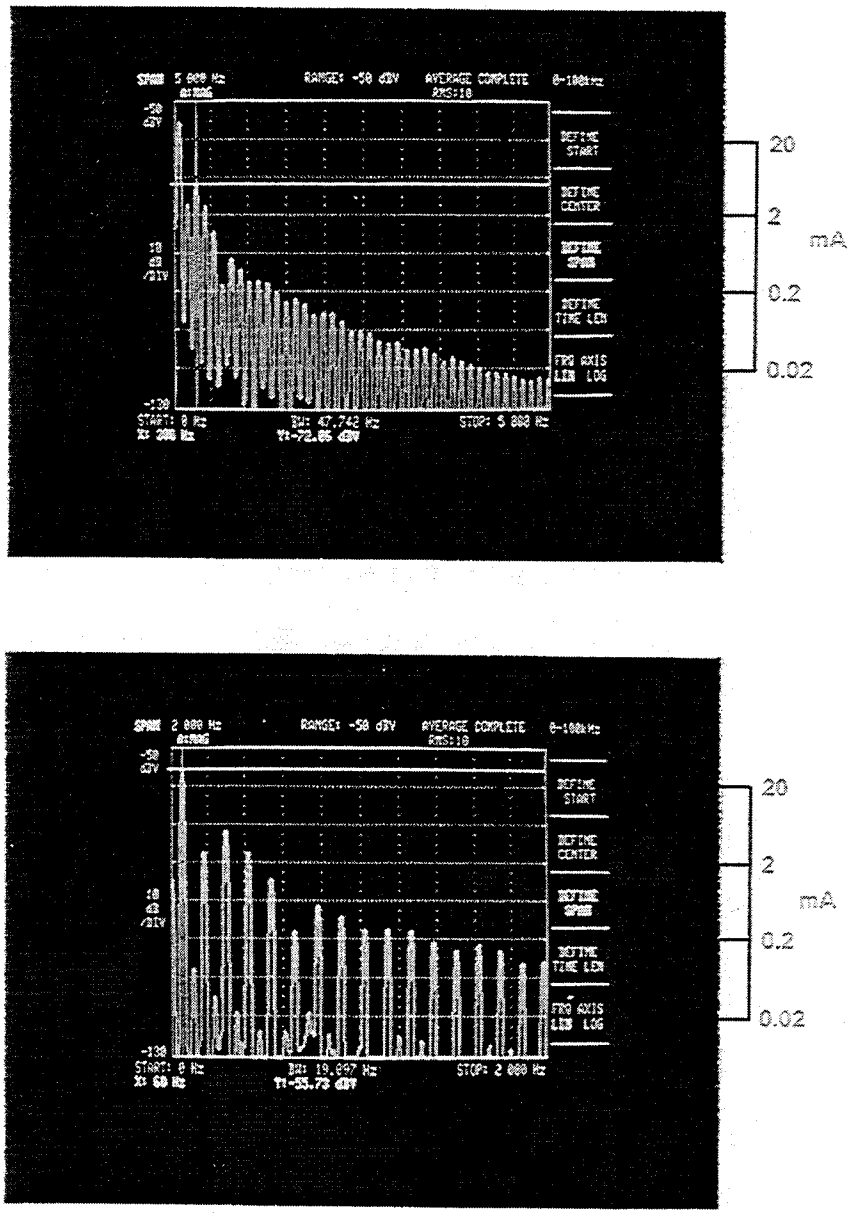

010501 1440
NPS. PL. 120VAC IN
CONTROL PWR ONLY
S. CT4(20/1), P6021(10/1), +20

Figure 3.1-2

LF Current, Black 120-VAC Conductor, Control Electronics Only

Only minor and insignificant differences are shown for the fundamental and harmonic currents flowing on the black and white conductors of the power cord. This suggests that the current in the safety ground (green) wire should be very low since it is the only significant path available for the return of unbalanced harmonic current for the frequency range shown.

Figure 3.1-3 shows the differential-mode current at 60 Hz and its low-order harmonics on the green conductor of the 120-VAC power cord when only the control electronics was operating. The top view shows spectral components up to 100 kHz. The bottom view shows an expanded view of the 60-Hz current and low-order harmonics up to 2 kHz.

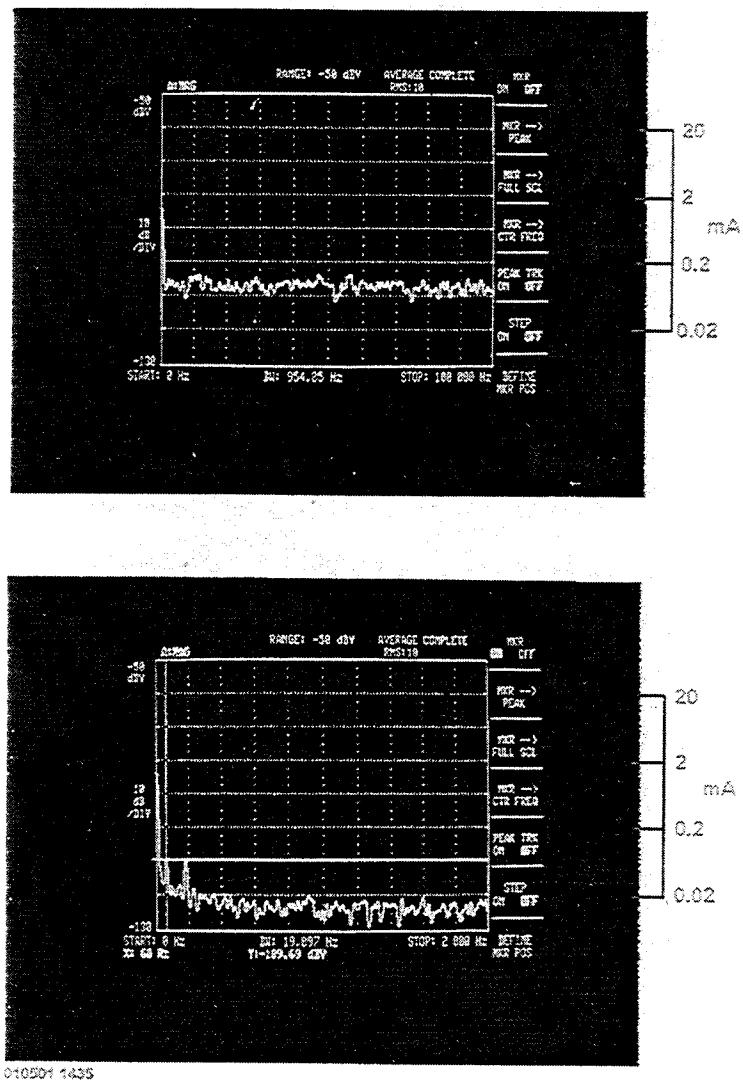

010504 1435
NPS, PL 120VAC IN
CONTROL PWR ONLY
G, CT4(20/1), P6021(10/1), +20

Figure 3.1.3

LF Current, Green Ground Conductor, Control Electronics Only

No significant amount of power-system harmonic current flows on the green-wire-ground conductor of the power cord over the frequency range of 200 Hz to 100 kHz. Only minor levels of current at 60 and 180 Hz are shown in the lower view of Figure 3.1-3. The level of both components was only about 0.06 mA and of no consequence.

Table 3.1-1 shows the scaled values of current flowing in the conductors of the 120-VAC power cord when only the control electronics was operated. The amplitudes of odd-order harmonics of the primary power frequency, and the fundamental and harmonics of the switching frequency are provided in the table. The amplitude of even-order harmonics was sufficiently low that they could be ignored.

Table 3.1-1

LF Current Amplitude, Control Electronics Only

Order Number	Frequency Hz	White mA	Black mA	Green mA
1	60	89.3	89.3	0.06
3	180	3.2	4.5	0.06
5	300	5.0	5.0	
7	420	2.8	2.8	
9	540	1.4	1.4	
11	660	0.2	0.2	
13	780	0.6	0.6	
15	900	0.4	0.4	
17	1020	0.3	0.3	
19	1140	0.3	0.3	
21	1260	0.3	0.3	
23	1380	0.2	0.2	
25	1500	0.1	0.1	
27	1620	0.1	0.1	
29	1740	0.1	0.1	
31	1860	0.1	0.1	
33	1980	0.1	0.1	

Next, the level of differential current flowing in conductors of the 120-VAC power cord was measured with the converter operating at full power. Figure 3.1-4 shows the current at 60 Hz and its low-order harmonics on the white conductor of the 120-VAC power cord. The top view shows spectral components up to 2 kHz. The bottom view shows an expanded view of the 60-Hz current and low-order harmonics up to 100 kHz.

The top view shows the fundamental and harmonic currents increased significantly over the prior measurements with only the control electronics in operation. The bottom view shows significant components at 21.4 kHz and at harmonics of that fundamental frequency. These components are produced by the switching rate of the power-conversion process.

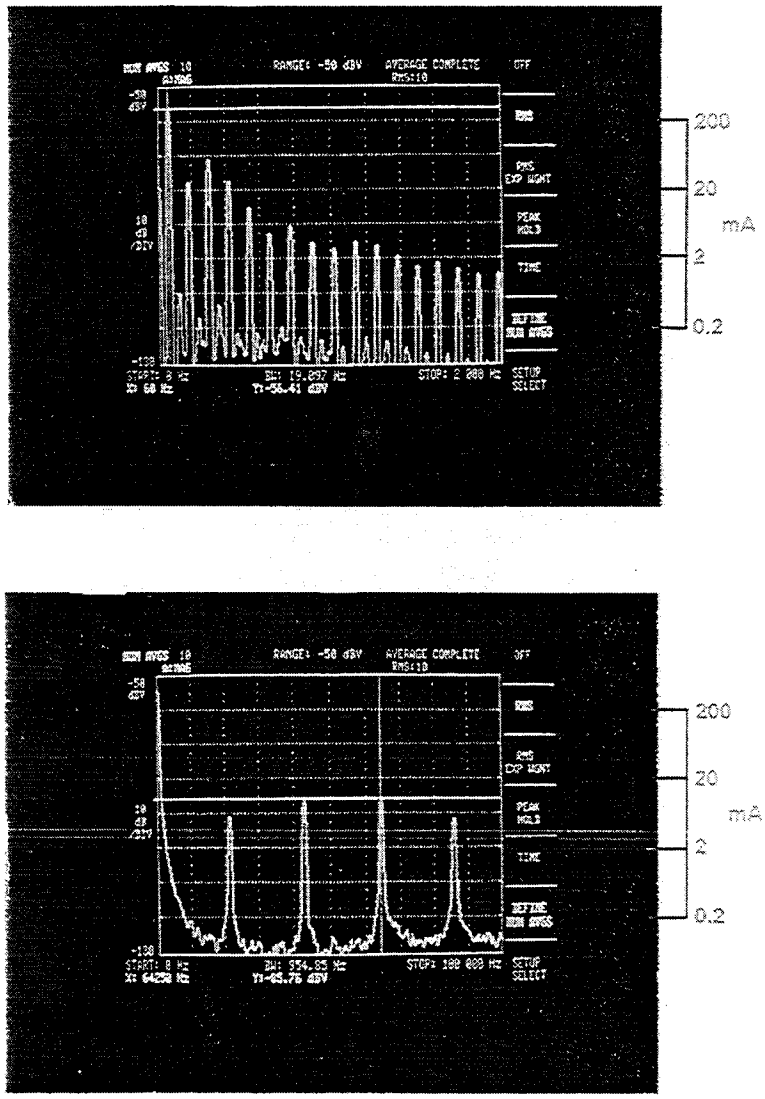

Figure 3.1-4

LF Current, White 120-VAC Conductor, Full Load

Figure 3.1-5 shows the differential-mode current at 60 Hz and its low-order harmonics on the black conductor of the 120-VAC power cord under maximum load conditions. The top view shows spectral components up to 2 kHz. The bottom view shows an expanded view of the 60-Hz current and low-order harmonics up to 100 kHz.

A comparison of the differential-mode current at 60-Hz and low-order harmonics shown in the upper views of Figures 3.1-4 and 3.1-5 indicates the black and white conductors carry about equal current levels below 2 kHz. A comparison of the lower views presenting the spectral components of the switching current shows the black conductor levels are significantly lower than the white conductor levels for the higher-frequency components produced by the switching rate of the converter. This suggests that significant unbalance current might be found on the green-wire conductor.

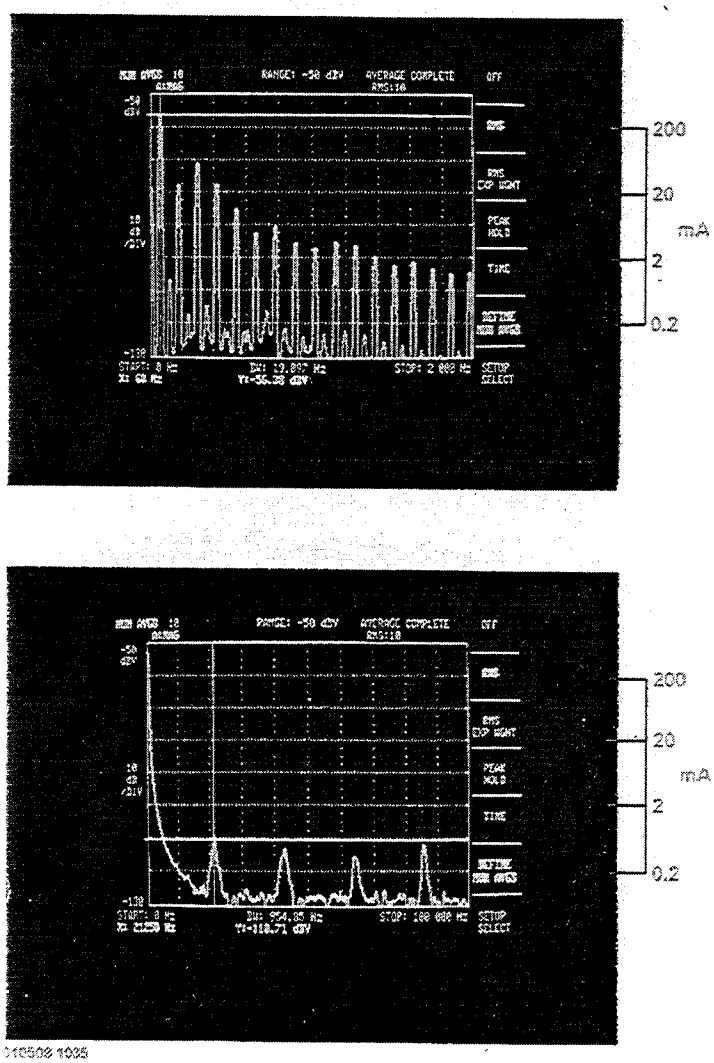

Figure 3.1-5

LF Current, Black 120-VAC Conductor, Full Load

Figure 3.1-6 shows the differential-mode current at 60 Hz and its low-order harmonics on the green conductor of the 120-VAC power cord under maximum load conditions. The top view shows spectral components up to 2 kHz. The bottom view shows an expanded view of the 60-Hz current and low-order harmonics up to 100 kHz.

As suggested by the white and black wire full-load current values, the green-wire current did increase somewhat compared to the very low levels found when only the control circuits were operated. The fundamental and harmonics of the switching rate of the converter appeared at higher levels.

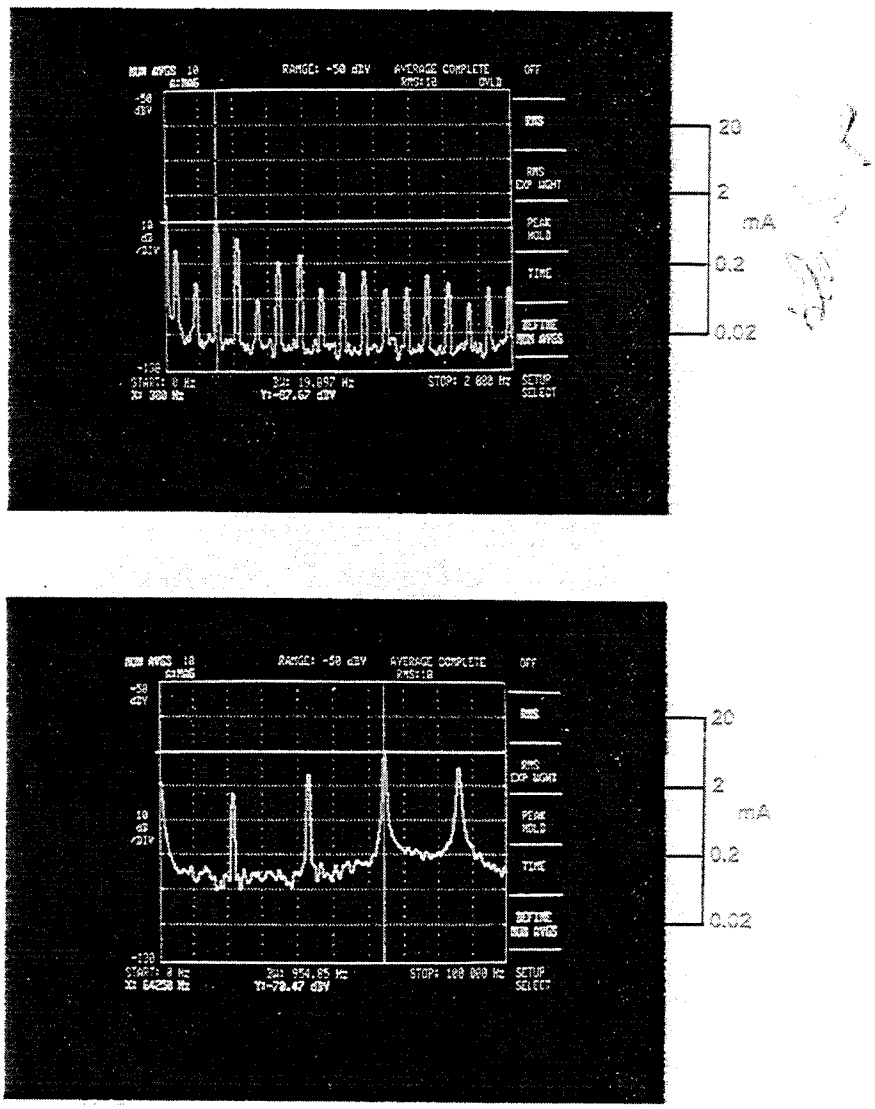

010502 102D
NPS, PL, 120VAC IN
400VDC @ 20.5A
G: CT4(20/1), P6021(10/1), +20

Figure 3.1-6

LF Current, Green Ground Conductor, Full Load

Table 3.1-2 provides the scaled amplitudes of the fundamental and harmonic currents flowing on the 120-VAC power conductors power conductors under full load conditions. The amount of current at the fundamental and harmonics of the switching frequency is shown at the bottom of the table.

Table 3.1-2

LF Current Amplitude, Full Load Operation

Order Number	Frequency Hz	White mA	Black mA	Green mA
1	60	710	710	0.3
3	180	31.7	31.7	0.1
5	300	56.4	63.2	0.8
7	420	25.2	25.2	0.5
9	540	12.6	11.3	0.2
11	660	5.0	5.0	0.3
13	780	5.6	6.3	0.1
15	900	3.6	3.2	0.2
17	1020	2.8	2.8	0.2
19	1140	3.6	3.6	0.1
21	1260	3.2	3.2	0.1
23	1380	2.0	2.8	0.1
25	1500	1.6	2.0	0.1
27	1620	1.8	1.6	0.1
29	1740	1.4	1.8	0.1
31	1860	1.1	1.3	0.1
33	1980	1.1	1.3	0.1
1	21400	5.6	0.6	1.6
2	42800	10.0	0.5	3.2
3	64200	10.0	0.3	6.3
4	85600	5.6	0.6	4.0

Low-frequency current flowing on the DC input and output conductors was measured to determine if spectral components existed at alternating-current frequencies. Figure 3.1-7 shows measured LF current on the input DC conductor for two levels of operation.

The top view of Figure 3.1-7 shows spectral components of current at 60 Hz and low-order harmonics up to 2 kHz with the converter operating at an input voltage of 412 VDC and 13.5 A. The bottom view shows the spectral component of current at 60 Hz and low-order harmonics up to 1 kHz with the converter operating at an input voltage of 500 VDC and 16.5 A.

The current at 60 Hz was very low for converter operation at a medium power level and even lower at the maximum operating level. Very high levels of current were found at the 3rd, 5th, and 7th harmonics. Harmonics below the 7th order decreased in amplitude as the power level was increased. The few data points available for harmonics above the 7th order show both increases and decreases. The data indicate that high levels of background noise also exist between the harmonics.

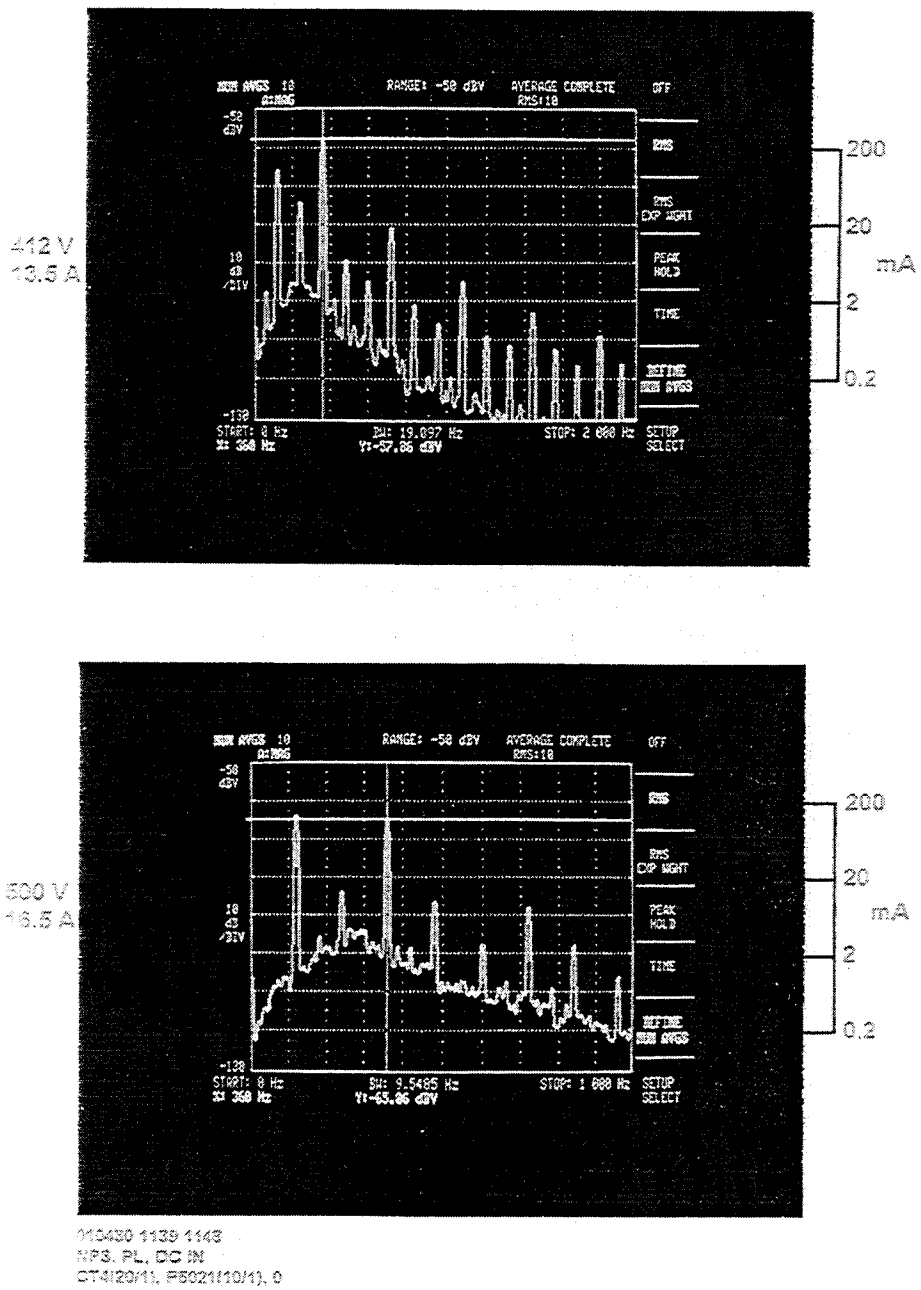

Figure 3.1-7

LF Current, DC Input Conductor, Two Levels of Operation

Figure 3.1-8 shows spectral components of current flowing on the input DC conductors over a 0-to-50 kHz frequency range with the converter operating at a voltage of 412 VDC and 13.5 A. The dynamic range of the instrumentation was barely sufficient to cope with the maximum current at low frequencies and also shows the spectral components of current at the higher frequencies. During this test the switching rate was determined to be 21,500 Hz, slightly higher than the rate shown in Figure 3.1-4. The switching rate was observed to vary during warm up and under some operational conditions, but the variations were small and of no consequence. The current at 21,500 Hz was 8 mA, and it was 2 mA at its second harmonic. No other component of current was found over the frequency range shown.

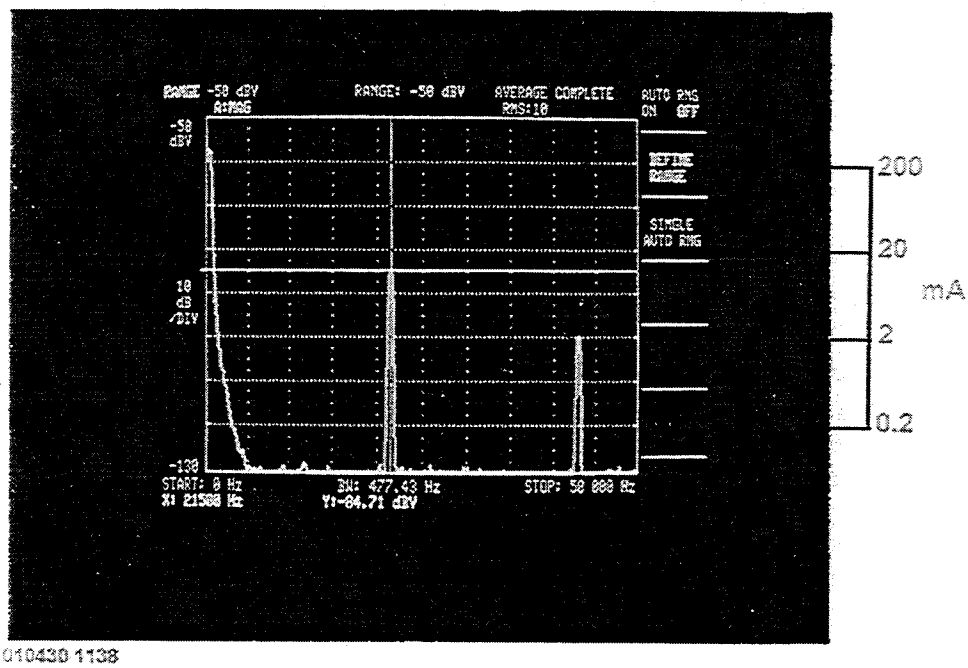

010430 1138
NPS, PL, DC IN
CT4(20/1), P6021(10/1), 0

Figure 3.1-8

LF Current, DC Input Conductor, 0-to-50 kHz

Table 3.1-3 provides scaled values of LF current for each primary component flowing on the DC input conductor at the fundamental and harmonics of the 60-Hz power used for the converter control circuits. Current at the even-order harmonics of 60 Hz was very low, and it was ignored. The amount of current flowing at the fundamental and harmonics of the switching frequency is shown at the bottom of the table.

Table 3.1-3

LF Current Amplitude, DC Input Conductor

Order Number	Frequency Hz	412VDC @ 13.5A mA	500VDC @ 16.5A mA
1	60	2.5	
3	180	224.4	126.2
5	300	63.2	12.6
7	420	251.8	112.5
9	540	6.3	8.9
11	660	3.6	2.5
13	780	17.8	8.0
15	900	2.0	2.5
17	1020	1.0	1.1
19	1140	3.6	
21	1260	0.6	
23	1380	0.6	
25	1500	1.3	
27	1620	0.5	
29	1740	0.3	
31	1860	0.6	
33	1980	0.3	
1	21500		12.6
2	43000		2.0

Figure 3.1-9 shows the spectral components of current on the output DC conductor over a 0-to-1 kHz range for two operating conditions. The top view shows the spectral components of current while the converter was operating at 320 VDC and 16.3 A while the lower view shows the current at 400 VDC and 20.5 A. Of interest is that the 2nd, 4th, 6th, and 12th even-order harmonics of the primary power system appeared on the output conductor along with the DC current as contrasted to the odd-order harmonics found on the other conductors. Higher-order harmonics of 60 Hz were below the measurement capability of the instrumentation, and they were considered insignificant for all practical purposes. Noise was found between the spectral components up to about 500 Hz.

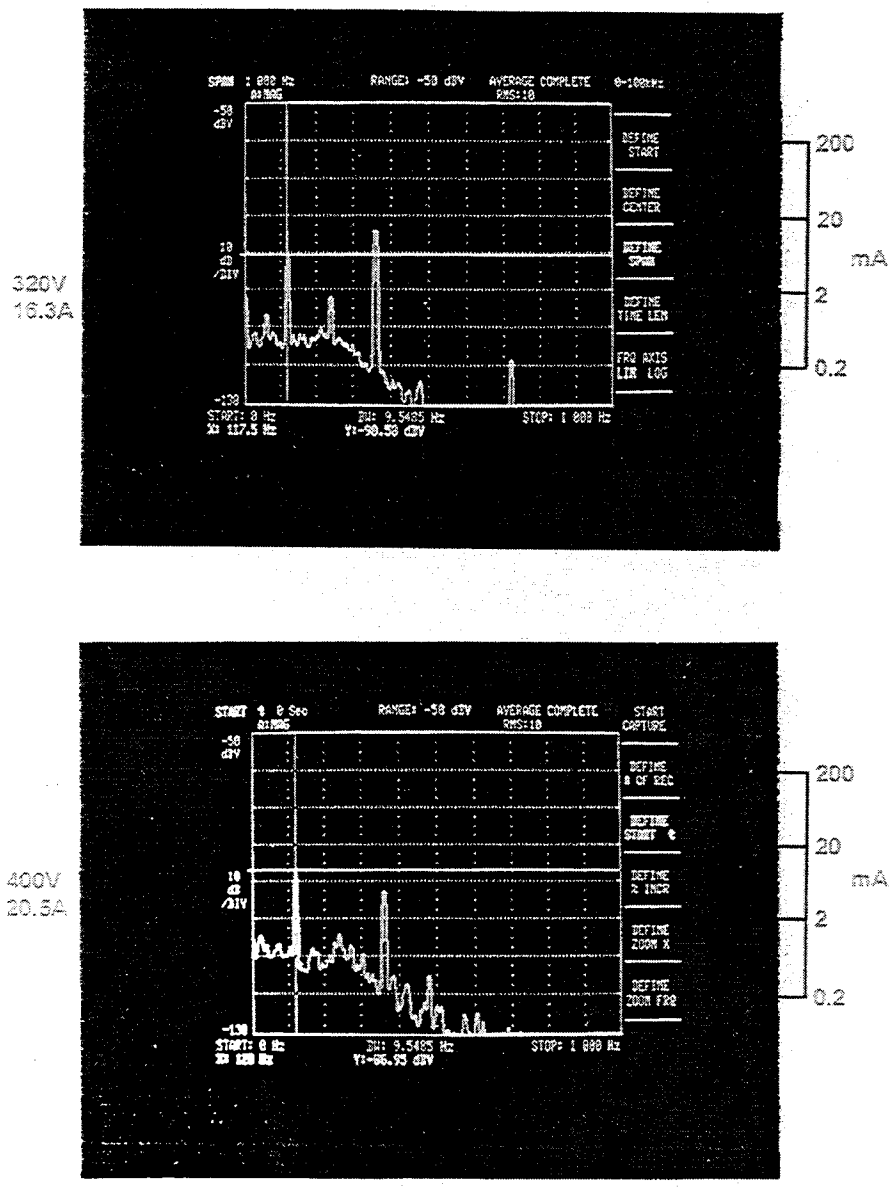

Figure 3.1-9

LF Current. DC Output Conductor, Two Levels of Operation

Figure 3.1-10 shows the spectral components found over a 0-to-50 kHz range. The switching frequency and its second harmonic are shown at significant levels. No other significant component of current was found. The gain of the analyzer was not sufficient to show the entire noise floor, but enough peaks in noise appear along the bottom of the view to indicate that no significant noise was present over the frequency range shown.

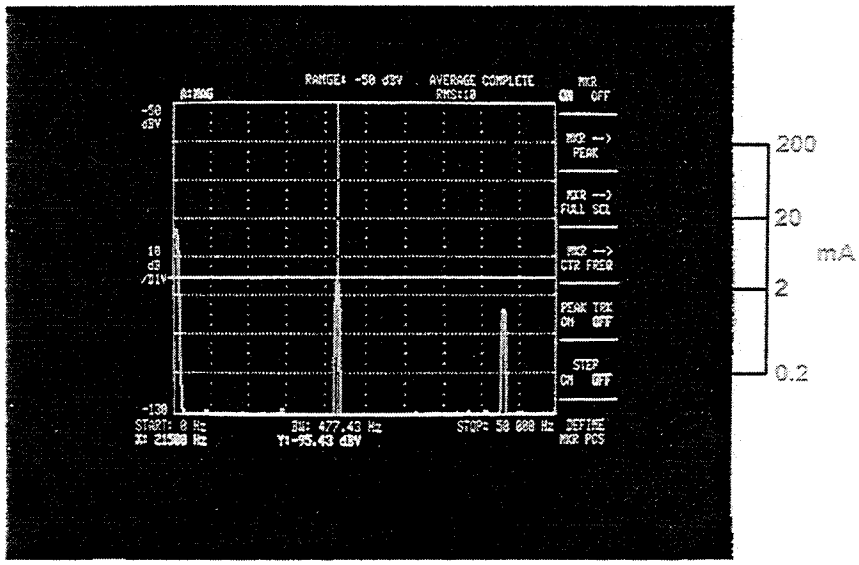

010430 1150
NPS, PL, DC OUT, 320V & 16.3A
CT4(20/1), P6021(10/1), 0

Figure 3.1-10

LF Current, DC Out, 0 to 50 kHz

Table 3.1-4 provides the amplitude of the primary spectral components of LF current found on the DC output conductor. The table includes the components found for the two levels of operation shown in Figure 3.1-9 at the low end of the LF range and the single level of operation shown in Figure 3.1-10 at the higher end of the LF range.

Table 3.1-4

LF Current Amplitude, DC Output Conductor

Order Number	Frequency Hz	300VDC @ 16.3A mA	400VDC @ 20.5 A mA
1	60	1.0	
2	120	2.0	8.9
4	240	1.6	
6	360	12.6	5.0
8	480	0.1	0.4
12	720	0.2	
1	21500		3.2
2	43000		1.3

3.2 High-Frequency Results

High-frequency data were obtained for the same two operating conditions used for the low-frequency measurements. These were when only the control electronics was operated and again under full power operation.

Figure 3.2-1 shows the differential-mode current flowing on the 120-VAC power-cord conductors when only the control electronics was operating. This provided a convenient starting point to understand the sources and magnitude of EMI current flowing on the white, black, and green-wire-ground conductors of the power cord.

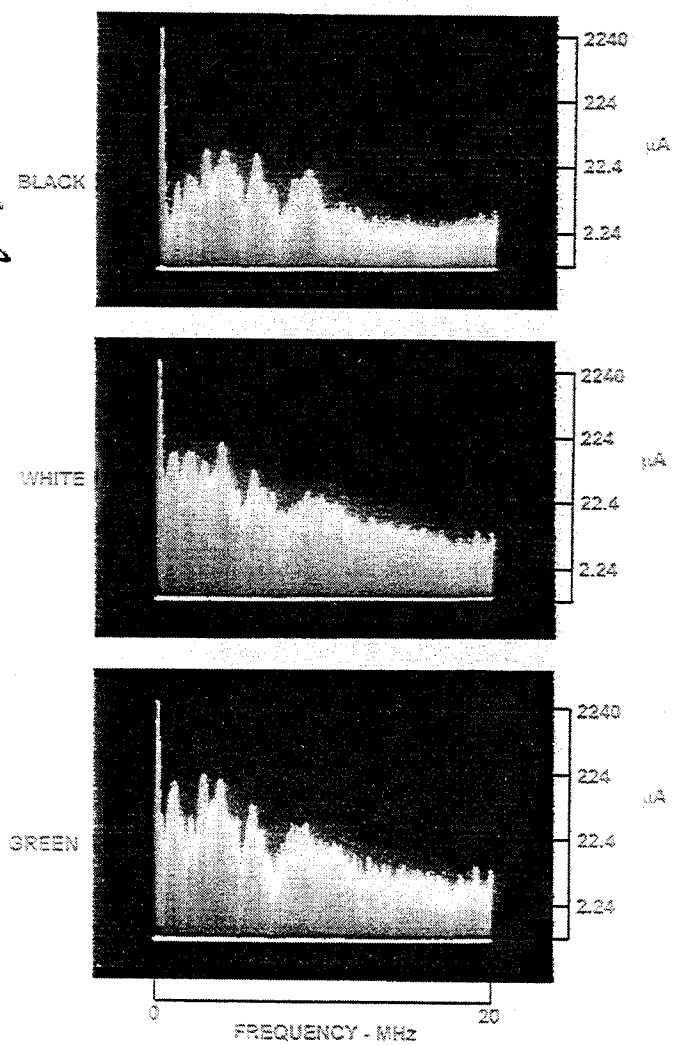

010501 1454
NPS. PL, 120VAC IN, CONTROL PWR ONLY
10M, 20M, 100k, 100ms
F-70, 0, 0, -30

Figure 3.2-1

HF Current, 120-VAC Conductors, Control Electronics Only

Figure 3.2-2 shows the differential-mode current flowing on the 120-AC power-cord conductors under full power conditions. The current levels on the white, black, and green conductors can be compared to the previous example when only the control electronics was operated.

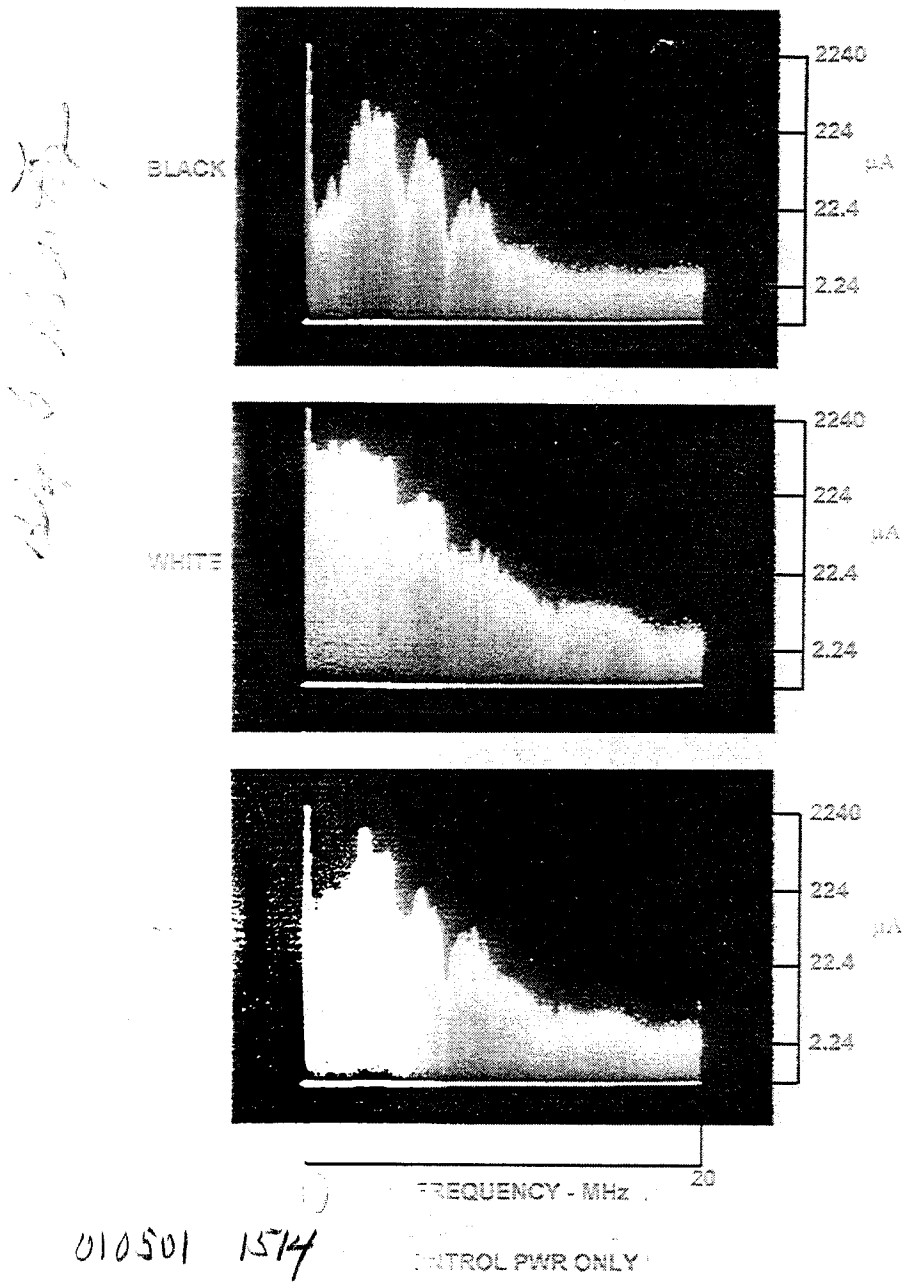

Figure 3.2-2

HF Current, 120-VAC Conductors, Full Load

Because of the complexity of the spectral shape of the high-frequency EMI current for the two operating conditions, it is difficult to provide a simplistic comparison of the two sets of data. The peaks and nulls in the spectral content of the HF current changed considerably from one operating condition to another. In addition, the spectral content of the white and black conductors was somewhat different indicating that not all of the current left the converter on the white power conductor and returned to its source on the black power conductor as noted during the LF measurements. In addition, the level of HF current injected into the green-wire ground system was sufficiently high to be of concern since a portion of this current will be injected into the ground conductors of other nearby equipment and into the facility ground conductors. Some of the green-wire current at the HF frequencies can also be returned to the converter by capacitive and inductive coupling to the other adjacent white and black power conductors, and this may account for some of the differences in the current flowing in the white and black conductors.

The HF current was considerably higher on all three of the 120-VAC power-cord conductors under full operating conditions compared to the current levels from the control power circuits. Of interest was that the HF current levels on the 120-VAC conductors gradually increased as the system load was increased, indicating that the HF current levels were related to the converter operating power level.

Next, the HF EMI current level flowing on the DC input conductor was examined. Figure 3.2-3 shows the HF current for maximum operating conditions.

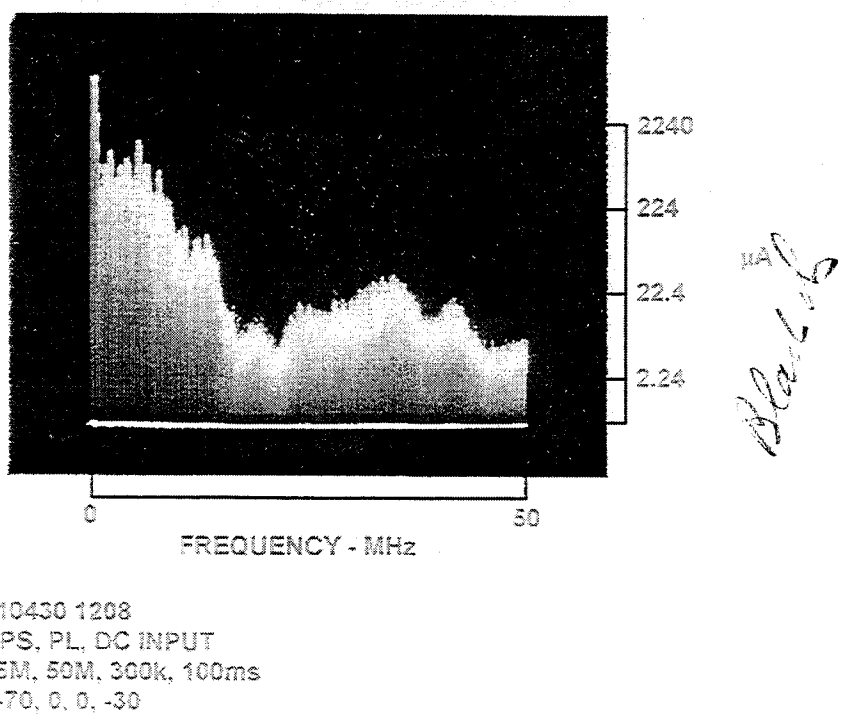

Figure 3.2-3

HF Current, DC Input Conductor, Full Load

The level of HF EMI current flowing on the DC output conductor was also examined under full operating conditions. Figure 3.2-4 shows the result of the measurement.

A very large peak in EMI current was found near the low end of the frequency scale at about 3 MHz. The amplitude of the current at this frequency was about 126 mA, a very high and undesirable level of EMI current. The amplitude decreased rapidly at higher frequencies and became quite low at and above about 15 MHz.

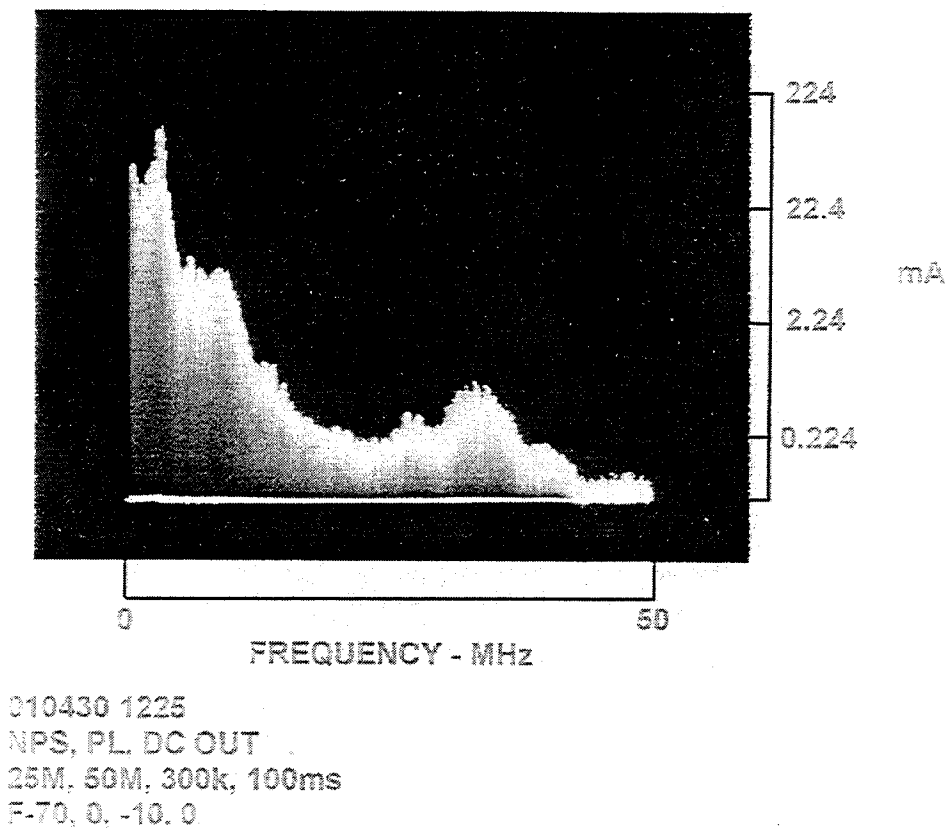

Figure 3.2-4

HF Current, DC Output Conductor, Full Load

4. DISCUSSION OF RESULTS

A large amount of data is included in the previous sections of this report in pictorial form and in a few summary charts. Many readers of this report will not wish to spend the time to examine the detailed data provided and to ascertain its use in the design and implementation of electric warships. This discussion, and the summary at the beginning of the report, provides a summary of the findings. ***In addition, the data provides a clear warning that power-conversion devices can and will adversely affect the operation of other systems and equipment on a ship unless early steps are taken to avoid the problem.***

A number of questions need to be asked concerning the data and its meaning. For example: What do the EMI results mean? Are the EMI current levels harmful or harmless? At what frequencies are EMI currents harmful and to what systems and what equipment? Do the levels exceed any meaningful specifications or standards? Will the EMI current cause any harmful impact on the operation of other systems and equipment on a ship or land facility? Will these EMI current levels scale up as power-conversion devices scale up as well? How much volume and weight should be allocated for EMI mitigation in electric warship architecture?

Before examining these questions, the team making the measurements must state that the use of solid-state power-conversion devices on a ship or in a land-based site provides many advantages over older technology. These devices provide new and valuable ways to control the flow of electricity, and this has significant implications for:

- the accurate and rapid control of electrical loads such as variable speed motor drives,
- the conversion of electric power from one type or level to another,
- the immediate control of the flow of electrical power from one user to a more critical user, and
- the temporary storage of electrical power.

Because of these advantages the plans to press ahead with an electric warship are fully supported. This report is part of an effort to understand some of the auxiliary problems that will be encountered by the use of power-conversion devices on ships and to develop solutions to those problems in a timely and cost-effective manner. It does provide a clear warning of an EMI problem that must be faced early in the design to avoid later costly retrofits.

Solid-state power-conversion devices are already appearing in land-based sites, and some versions have started to appear on ships for auxiliary and secondary applications. These devices will rapidly increase in numbers and applications since they already solve a number of key operational problems, and they will solve many more in the next few years. But this introduction, if not carefully implemented, will likely result in harmful levels of electromagnetic interference to communication and navigation systems and cause the erratic operation and malfunction of some data-processing systems. This has already happened and been documented in land-based sites, and costly corrective actions

are a result of not understanding all of the implications of the EMI generated by such devices.

The first step in understanding the problem is the determination of: "what is a harmful level of EMI current, voltage, or power?" This is not an easy question to answer since EMI is usually a very broad-band phenomenon, and the paths from a source of EMI to a victim of EMI are often poorly understood, largely ignored, and highly variable from one case to another. The susceptibility of victim equipment to EMI is also highly variable, and it is different from one device to another, particularly with COTS equipment. Nevertheless, a start at answering this question has been provided by a series of EMI leakage measurements made in land-based radio and data-processing facilities. These measurements determined the limits of EMI current that can be tolerated in such facilities without generating harmful interference to operating systems. It was found that existing land-based receiving facilities are susceptible to very low levels of EMI current flowing on power-system conductors, power-system safety-ground conductors, coaxial-cable shields, data-cable shields, and facility grounds[4]. Table 4-1 summarizes the threshold limits of EMI current that were found to limit the ability of small and large radio receiving sites to receive radio signals without encountering harmful levels of interference. The limits shown in this table are very small. Reasonable values for the region between 10 kHz and 100 kHz can be obtained by the linear scaling of the data between the two points.

Table 4-1

Maximum Tolerable Levels of EMI Current in Shore Facilities

Frequency Range	Large Facility Maximum Current	Small Facility Maximum Current
100 Hz to 10 kHz	2 mA	2 mA
100 kHz to 100 MHz	10 μA	2 μA

While the tolerable levels of current can be increased somewhat above the limits provided in Table 4-1 by improved system and equipment installation practices, the direct radiation of EMI from conductors in a facility, or a ship, directly into antennas is a key limiting factor.

Unfortunately, similar data to that in Table 4-1 is not yet available for ships. The small amount of information obtained from limited work on two ships suggests that present day electrical and physical equipment installation practices on ships will probably result in similar results. This kind of information must be obtained from ships before reasonable limits can be set for conducted EMI. The vulnerability of existing communication, navigation, and data-processing systems to EMI generated by power-conversion devices can be determined by relatively simple shipboard measurements. This is not a complex task, and it can be accomplished during the normal operation of a ship.

[4] Wilbur R. Vincent, Richard W. Adler, and Hugh J. Myers, ***EMI Leakage into the Radio Frequency Distribution System of a Receiving Site***, Technical Report WAH9607A, Prepared for Commander COMNAVSECGRU, N-44, January 1997

Once the tolerable limits of EMI current are established, the next step is to develop and apply the techniques needed to limit the levels of EMI current to these limits. This report is one small step in that process. It also provides some of the information needed to develop mitigation techniques for power-conversion devices up to about 100 kW and provides some of the information needed to develop a model to predict the levels of EMI current to be expected from higher-power converters.

The data in this document provide a number of interesting results about levels of conducted current than can be expected from low-power devices unless precautions are taken. These are highlighted as follows:

LF current on the 120-VAC power conductors with only control circuits operating:. Digital power-conversion devices usually inject harmonics of the power frequency and high-frequency EMI current into the green-wire safety-ground conductor as well as into the black and white conductors. In this case, the control electronics did not inject any significant level of harmonic current into the green-wire conductor (see Figure 3.1-3). Low impedance paths were obviously provided for this current to return to its source within the converter before the green-wire ground connection was reached. The power supply for the control electronics did inject significant levels of odd-harmonic current into the white and black power conductors, and this is normal for many types of switching power supplies. The amplitude of the odd harmonics is not excessive for the device examined.

LF current on 120-VAC power conductors under full operation:

LF current on the white, black, and green conductors of the power cord during full operation of the converter reached levels of some concern. While the harmonics of the power frequency remained at acceptable levels, the fundamental and harmonics of the converter's switching frequency increased sufficiently to become of concern (see Figure 3.1-5). The 60-Hz current increased from 89.3 mA to 710 mA and harmonics increased by about the same ratio. While the levels of harmonic are not of concern for this converter, they indicate that a higher-power device will generate higher and unacceptable levels of harmonic current.

HF EMI current on 120-VAC power conductors with only control circuits operating: The level of HF EMI current flowing on the power conductors and on the green-wire safety-ground conductor was well above the acceptable limits for land-based sites and probably would result in interference to radio communication and navigation systems operating at frequencies below about 50 MHz. A standard commercially available and inexpensive power-line filter, properly configured and installed, should correct this problem. If properly specified, a filter could also reduce the level of the LF current at the switching rate to acceptable levels, and it might also provide a path for some of the LF harmonic current to return to its source inside the converter case.

LF Current on the DC input conductor: Excessive levels of current were found on the DC input conductor at harmonics of 60 Hz and at the converter switching frequency and its harmonics (see Figure 3.1-7).

HF Current on the DC input conductor: Excessive levels of HF EMI current were present on the DC input conductor.

HF Current on the DC output conductor: Exceptionally high levels of HF EMI current were found on the DC output conductor during full operation (see Figure 3.2-4). The components of EMI current on all conductors entering and exiting the DC-to-DC converter during full operation exceeded levels suitable for land-based facilities. This current can be conducted and inductively and capacitively coupled to other conductors, grounds, cable shields, equipment cases, and structural material of ships and fixed facilities. The excessive levels of EMI current flowing on conductors penetrating the housing of the converter greatly increase the chance of leakage into victim devices and disrupting operation of electrical and electronic systems. Standard EMI containment techniques can be used to correct this problem at operating levels up to about 100 kW although they become physically large, heavy, and require cooling at high power levels. ***These volume and weight considerations must be addressed early in the design of the electric warship by the naval architects if costly retrofit to correct EMI problems is to be avoided.***

Of concern is that the EMI current increases in level as converter operating power increases although the scaling rules are not yet established. The data provided clearly indicates that a higher-power device will be a major source of interference to communication, navigation, and data-processing systems and perhaps even to other power-conversion devices. Of additional concern is that COTS EMI mitigation components and techniques are not presently available to correct EMI problems at operating power levels above about 100 kW.

A number of tasks must be implemented in order to ensure that power-conversion devices can be used on ships. These are:

- Conduct shipboard measurements on the susceptibility of present communication, navigation, and data-processing systems to the levels of EMI expected from medium to high-power conversion equipment. This can be accomplished during normal operation of such systems by injecting test EMI signals into power conductors, cable shields, and grounds at low levels and examining the leakage into operation systems. This type of information is required to establish reasonable levels for the maximum tolerable levels of EMI current for ships.

- Make conducted EMI current measurements on higher-power devices. The test bed at the Philadelphia Naval Shipyard provides an excellent place for such measurements. No modification of the test bed is required, and such measurements can be conducted during normal test runs of the present power-conversion devices.

- Collaborate with converter design personnel to implement circuit changes that will provide low-impedance conducting paths for the return of EMI current to its source inside the converter housing and high-impedance paths to conductors penetrating the converter's housing.

- Investigate multiple-stage filters for high-power use that will provide high-impedance paths preventing the escape of harmful levels of EMI current from the converter housing while not interfering with the normal transfer of electrical power. Apply these designs in a Barrier, Filter, and Ground configuration for optimum effectiveness and minimum size.

INITIAL DISTRIBUTION LIST

		No. Copies
1.	Defense Technical Information Center 8725 John J. Kingman Rd, STE 0944 Ft. Belvoir, VA 22060-6218	2
2.	Dudley Knox Library, Code 52 Naval Postgraduate School 411 Dyer Road Monterey, CA 93943-5101	2
3.	Research Office, Code 09 Naval Postgraduate School 589 Dyer Road Monterey, CA 93943-5138	1
4.	Chairman, Code EC Department of Electrical and Computer Engineering Naval Postgraduate School 833 Dyer Road Monterey, CA 93943-5121	1
5.	Andrew A. Parker, Code EC/Pk Department of Electrical and Computer Engineering Naval Postgraduate School 833 Dyer Road Monterey, CA 93943-5121	4
6.	Richard W. Adler, Code EC/Ab Department of Electrical and Computer Engineering Naval Postgraduate School 833 Dyer Road Monterey, CA 93943-5121	4
7.	Wilbur R. Vincent, Code EC/Ab Department of Electrical and Computer Engineering Naval Postgraduate School 833 Dyer Road Monterey, CA 93943-5121	4

		No. Copies
8.	Robert W. Ashton, Code EC/Ah Department of Electrical and Computer Engineering Naval Postgraduate School 833 Dyer Road Monterey, CA 93943-5121	1
9.	John G. Ciezki, Code EC/Cy Department of Electrical and Computer Engineering Naval Postgraduate School 833 Dyer Road Monterey, CA 93943-5121	1
10.	Bryan D. Whitcomb, LT, USN. Department of Electrical and Computer Engineering Naval Postgraduate School 833 Dyer Road Monterey, CA 93943-5121	1

Multiple GPS RFI Sources in a Small California Harbor

James R. Clynch
Department of Oceanography, Naval Postgraduate School,
Andrew A. Parker, Richard W. Adler, and Wilbur R. Vincent
Department of Electrical and Computer Engineering, Naval Postgraduate School
Paul McGill and George Badger, Monterey Bay Aquarium Research Institute

BIOGRAPHY

James R. Clynch has been a Research Professor at the Naval Postgraduate School since 1990. Prior to that he was at the Applied Research Laboratories, University of Texas at Austin for 18 years. He has worked for the past 30 years in the use of satellite navigation systems for precision positioning and to study propagation effects.

Andrew A. Parker, Richard W. Adler, and Wilbur R. Vincent are Research Professors in the Department of Electrical and Computer Engineering at the Naval Postgraduate School, Monterey, CA. They are active in work on electromagnetic signals.

Paul McGill is an Electrical Engineer and George Badger a Microwave Technician at the Monterey Bay Aquarium Research Institute. Mr. Clynch has a PhD from Brown University, Mr. Adler a PhD from Pennsylvania State University, Mr. Parker a MS from the University of Maryland and Mr. Vincent a MS from Michigan State University.

ABSTACT

After receiving multiple reports of GPS being jammed in and around the Moss Landing, CA harbor, an effort was mounted by the Naval Postgraduate School (NPS) and the Monterey Bay Aquarium Research Institute (MBARI) to locate the source. Jamming was reported both inside and outside the harbor. MBARI has a differential GPS station at their Moss Landing headquarters to support their research vessels docked there. Logging of the MBARI DGPS corrections established continuous jamming of their Trimble reference receiver. Many other receiver types were also jammed in the harbor. Three sources were eventually located. Spectra taken in the field as well as laboratory test results on the highest level source will be reported.

The first, highest level, jamming was located and found to be a Radio Shack VHF/UHF marine TV antenna with a built in pre-amplifier. The unit was on a small fishing boat. It was purchased from the owner and extensively studied in a laboratory. It had a parasitic oscillation at the GPS frequency that was very sensitive to the presence of nearby metal objects, power-supply-voltage fluxations, electromagnetic fields from nearby building wiring, electromagnetic fields from VHF hand-held transceivers, and other things. The unit was forwarded to the FCC.

Jamming of GPS still occurred in Moss Landing, but only at night. This was found to be correlated with external temperature. MBARI, NPS and the FCC searched for this unit. It was called Source-2. They quickly found a third RFI emitter that was a Shakespeare active VHF/UHF TV antenna. It appears the unit was manufactured at the same factory. This was called Source-3. The FCC got this source deactivated and continued searching for Source-2, eventually locating it.

The levels at the MBARI site for the three sources were calculated. Source-1 (Radio Shack Antenna) had a level of -96 dBm. Source-2 varied in frequency and level. While on top of L1 it had a level of -106 dBm. Source-3 (Shakespeare Antenna) had a level at MBARI of -99 dBm. Source level cannot be computed because the signals suffered an unknown amount of attenuation going through a building and/or their location is unknown. The Source-1 to MBARI range was 325 m at an elevation angle of - 2.5 degrees.

INTRODUCTION

The Captain of a 500 ton research vessel based in Moss Landing, CA made a radio telephone to call one of the authors (Clynch) in early April 2001. The captain stated that the whole of Moss Landing Harbor was jammed. He was advised to contact the US Coast Guard (USCG) and the Federal Communication Commission (FCC). When

the problem persisted for another month, an effort was made on the local level to determine the cause of the jamming. This was successful and an active TV antenna was located and removed. Soon afterward it was found that jamming was still present. This lead to a continued search with 2 additional sources being identified.

Moss Land is a moderate size harbor about 100 km south of the San Francisco. It has a mixed fleet of working fishing boats, pleasure craft and three large research vessels used by the local science community. Location of the harbor, in the middle of Monterey Bay is shown on the map in Figure 1. The Naval Postgraduate School (NPS) is located at the south end of Monterey Bay. NPS has a large program in science and engineering. The work in GPS is done mainly by Mr. Clynch of the Oceanography Department. Messrs. Adler and Parker are part of a Electrical Engineering group specializing in electromagnetic signals.

The Monterey Bay Aquarium Research Institute (MBARI). MBARI is headquartered in Moss Landing and has two major research vessels berthed there. This organization, founded by David Packard, not only supports the Monterey Bay Aquarium, but also has a fairly large engineering program, especially in underwater remotely operated vehicles. They are responsible for data links that send video from at sea work to the Aquarium for viewing by the visitors there. To support this they have a small cadre of engineers, including Messrs. McGill and Badger, experienced in radio communications. Mr. Gary Thurmond recently retired from MBARI where he was responsible for the design of the radio communications systems.

MBARI has used GPS for precision location of their vessels since the early 1990's. This was before the USCG set up their system of DGPS stations along the coast. MBARI, with assistance from NPS, set up a differential station at their location at Moss Landing. This was based on a Trimble RL 4000 GPS receiver. They used a UHF data link to send the corrections to their vessels. After the jamming report was received in April, NPS set up a monitor of the MBARI DGPS corrections to log the number of satellites being tracked. This clearly showed that the station was being heavily jammed. Reports of other GPS users in Moss Landing confirmed that it was a jamming issue and not a faulty receiver.

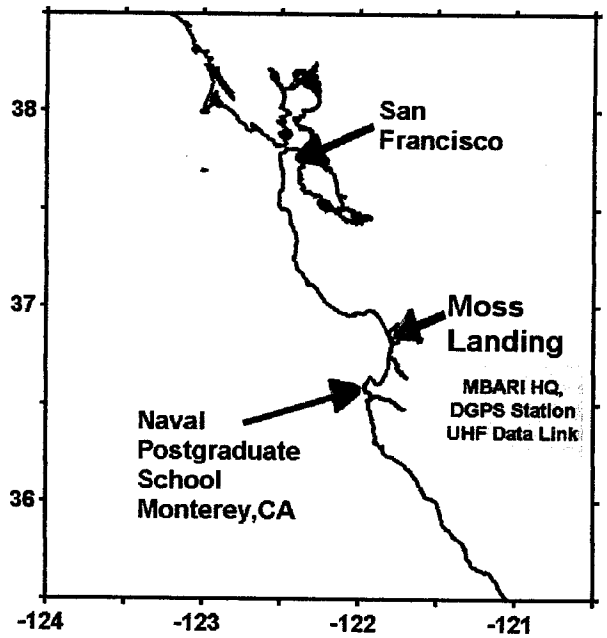

Figure 1

The GPS signal that feeds the MBARI reference station was also distributed to several laboratories and offices in the MBARI headquarters building. This was done through a series of splitters and inline amplifiers. In an office with one of these drops a high quality spectrum analyzer (HP 8562 A 0 – 22 GHz) was set up to examine the spectrum near L1. The signal were uncalibrated. Figure 2 shows an example of the data recorded with a clear peak from the RFI source many dB above the level of the GPS signals.

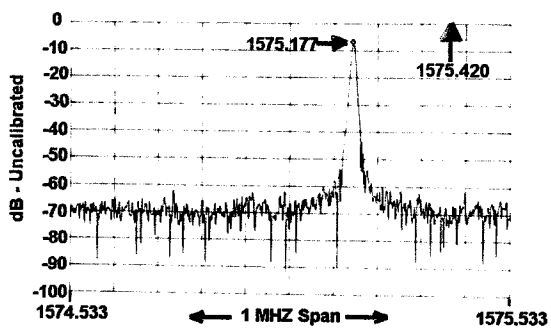

Spectrum Of Source I

HP 8562A Spectrum Analyzer
VBW 3 KHz RBW 3 KHz

Figure 2

IDENTIFICATION OF SOURCE I

The search for the source of the jamming radiation was begun in early May, 2001. It was carried out mainly by engineers from MBARI, Mess. McGill and Badger, along with Mr. Thurmond. They spent several days looking for the source. The search was complicated by two factors: the large number of metal objects that reflected the energy and the shifting of the frequency of the emitter.

Mr. Badger fabricated a 17 element yagi antenna and used this with a small portable receiver (Icom IC-R3 5). The initial search drove along the roads in the area and stopped at widely spaced locations to record the peaks of the RFI signal. There were multiple peaks in all locations. These came from the multitude of reflecting structure in the area, including the largest conventional power plant in California.

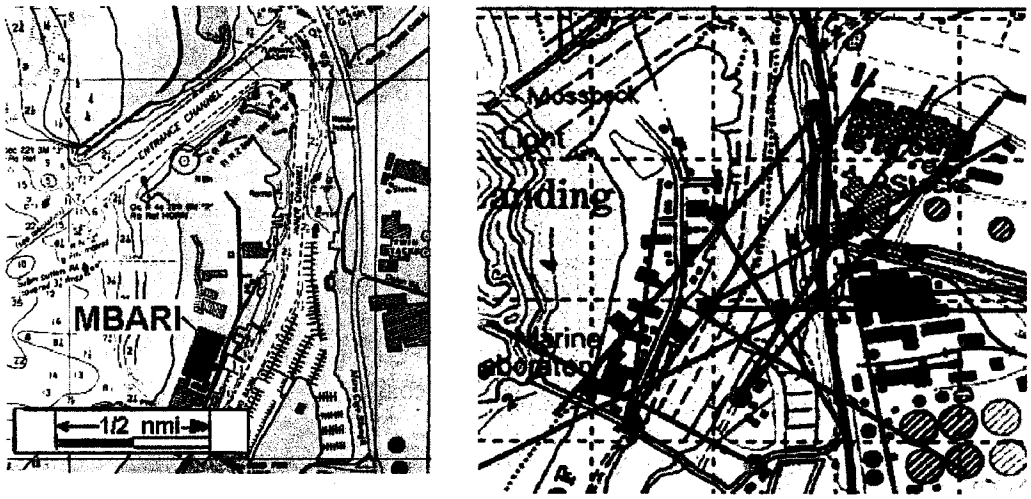

Source I Search Bearings

Figure 3

The left map in Figure 3 shows the southern half of Moss Landing Harbor. The right half shows the locations where bearing were taken as green circles and the bearings in blue. The red circle was the location of the emitter. Without the red dot, it is hard to define where the most likely position is. After ruling out the power plant it was decided to look where there were no building or other reflectors.

The spectrum analyzer was put on a cart and along with the small radio taken to the dock area. Even then it was confusing. Only by turning off shore power to boats could the actual emitter location be determined. The picture if Figure 4 was taken by Mr. Thurmond from a "kite camera" at about 200m. It shows the location of the RFI emitter, MBARI, and the power plant.

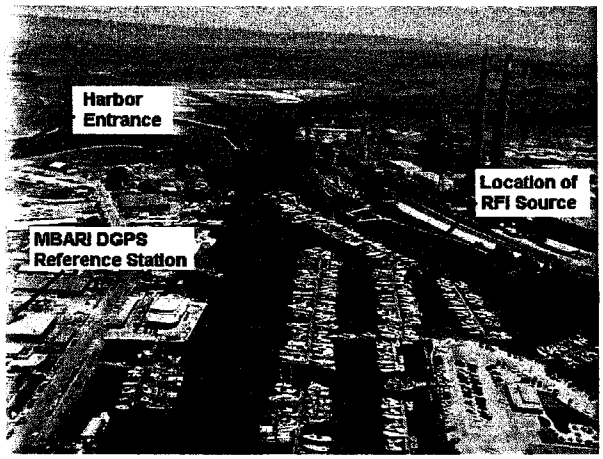

Moss Landing, CA Harbor
GPS RFI Source May 2001

Figure 4

The owner of the boat was contacted. With access to the boat it was quickly determined that the emitter was a Radio Shack VHF/UHF TV antenna with built in preamplifier. The antenna was powered by an AC/DC adapter plugged into boat AC power. The preamplifier was thus powered all the time, even when the TV was not on. In fact, the TV was seldom on and most of the time the TV antenna was in a paint locker inside the locked boat. From this interior location, shown in Figure 5, the emissions were jamming all of Moss Landing Harbor and an area at least 1 km out to sea.

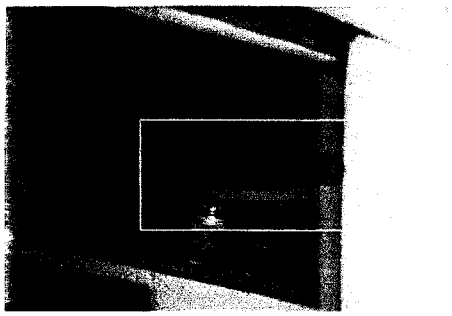

Active UHF/VHF Antenna In Small Ship Paint Locker

Figure 5

The day after the TV antenna was located, it was purchased from the owner and taken to NPS for study. It was a Radio Shack model 15-1624. The Federal Communications San Francisco Field Office was informed of the find. A memorandum [Clynch 2001] describing the facts of the case was also distributed to the US Coast Guard, and the GPS JPO.

CHARACTERISTICS OF SOURCE I

The antenna was brought to NPS for study under controlled conditions. It was found to have an internal preamplifier that exhibited parasitic oscillations. The unit was normally powered from a 12 volt, inexpensive AC/DC converted. In the tests it was powered from both this unit and a battery. The unit is shown in Figure 6 with the cover closed and open. The small preamplifier that was jamming GPS is evident.

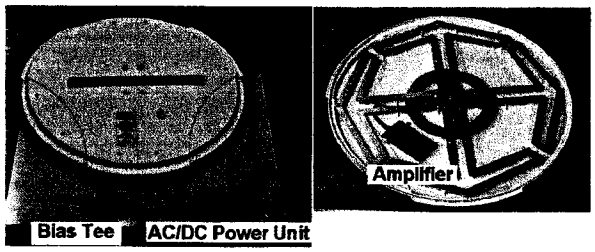

Radio Shack 15-1624 VHF/UHF Antenna

Figure 6

The characteristics of the emission were studied using a HP 8562E spectrum analyzer with its output sent to a waterfall display.

The unit was extremely sensitive to the physical and electrical environment. This was known from the search when modulation on the signal was recognized a boat sump pump. At one point it was noted that the frequency varied over 3 MHz when a hand was slowly moved a few cm when it was 3 m from the antenna. This is shown on the left in Figure 7. When the hand was held still the frequency was much more stable as seen by the section at the top of the traces.

In another case, when running on batteries, the spectral pattern changed considerably when the overhead fluorescent lights were turned on and off. This effect is shown in the figure on the right. In order to get the narrow lines in the "lights on" condition, the spectrum analyzer was synchronized to the AC line frequency.

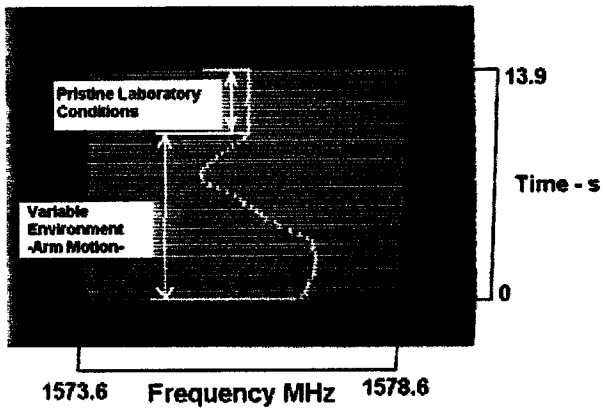

Frequency Change From Nearby Hand

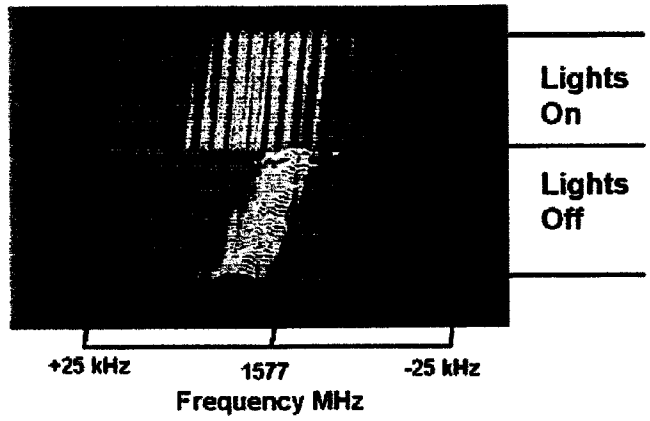

EM Coupling - Fluorescent Lights

Enviromental Effects

Figure 7

In order to investigate the electromagnetic coupling better, the unit was placed in a good screen room. It still oscillated indicating that the oscillation was self excited. It was also found that the operation of a low powered hand-held transceiver (100 mW) operation at 150 MHz and 450 MHz caused large shifts in the oscillation center frequency.

Several other tests results were obtained [Parker et. al, 2001], but the main result was that the oscillation was self exciting and very sensitive to environmental conditions.

MULTIPLE RFI SOURCES

During the hunt for RFI Source-1, NPS monitored the DGPS corrections broadcast by MBARI. The total number of satellites for which corrections were generated was automatically recorded and plotted every few days. While Source-1 was active, there were no satellites being tracked.

A few days after Source-1 was removed, this log was again plotted. Unfortunately there were still long periods when the MBARI GPS receiver was tracking few or no satellites. The MBARI GPS receiver was being jammed during most nights. A plot of the number of satellites tracked is shown below.

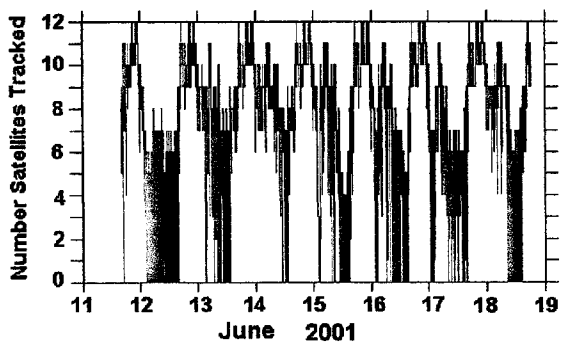

Source-2 Jamming of MBARI DGPS

Figure 8

It was conjectured that the jamming had the diurnal pattern due a the temperature sensitivity of the center frequency. This turned out to be partially correct. A plot of the temperature recorded in the Moss Landing Harbor is shown below. The times when the jamming from Source-2 were occurring over several hours a day are marked.

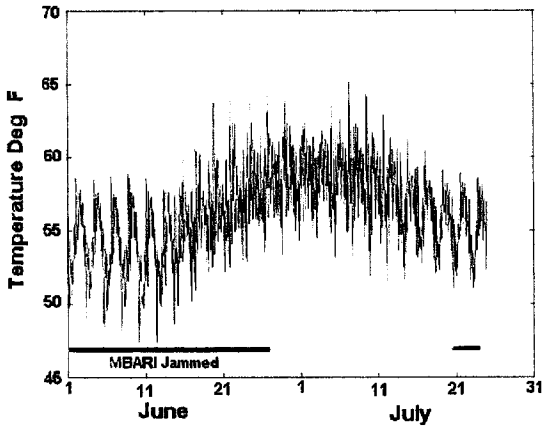

Moss Land Harbor Temperature
Days MBARI Jammed at Night

Figure 9

This meant that the source location hunt might have to be conducted at night.

The San Francisco FCC field office sent a team several times to Moss Landing to hunt for this RFI source. On several of the days both MBARI and NPS assisted. The signal was monitored in the MBARI building on the high quality spectrum analyzer. The frequency was seen to move during the morning hours and the level decreased as the temperature rose. The frequency was sent via cell telephone to the team in the harbor looking for the RFI source. A typical early morning spectrum is shown in Figure 10. This spectrum was taken after Source-1 was removed.

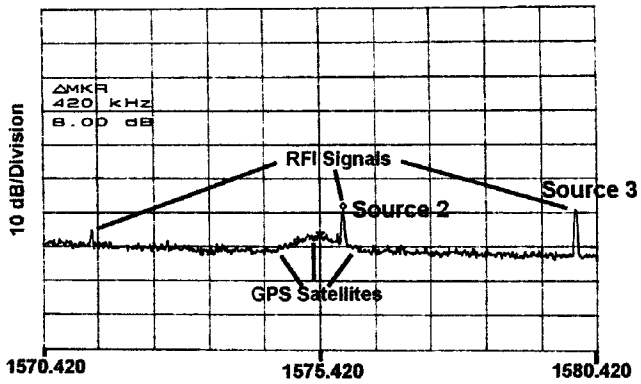

Spectrum at Mbari
4 June 2001 After First RFI Source Removed

Figure 10

Several signals are visible in this spectrum. In addition a broad peak in the middle from the GPS satellites is visible. This was not seen in the spectra taken earlier because Source-1 mask it. The peak in the GPS band is from Source-2.

On the second FCC trip to Moss Landing Harbor, the signal in the GPS band had dropped by 10 dB in the late morning. It was decided to hunt the source of the line about 1580 MHz. The combined group located this quickly. It turned out to be a Shakespeare UHF/VHF TV antenna on a boat one dock over from Source-1. When it was turned off, only the line near 1580 MHz went away. Therefore it was labeled Source-3. This unit was returned by the owner to the place of purchase for a replacement.

The FCC has determined that the preamplifiers in Source-3 and that in the Radio Shack antenna were from the same factory. This factory, owned by a subsidiary of Tandy, sold units at least to Radio Shack, Shakespeare, Thompson, and RCA. It is believed that the bad units began with a design change in late 2000. The number of units sold is not known to the authors.

It is now clear that there were at least 3 signals capable of jamming GPS in the Moss Landing Harbor area. Two were located and removed by a coordinated effort of MBARI, NPS and the FCC. The FCC made a few more attempts to locate Source-2 during the summer, but its level was lower with the higher temperatures. In the fall of 2001, the FCC located Source-2.

CALIBRATION

There were a large number of spectra taken in the MBARI office. The signal came in the Trimble antenna and went through two splitters and one inline amplifiers in the approximately 80 meters of low loss cable before emerging in the engineering office. Rather than examining the individual elements, it was decided to calibrate the entire system.

A calibrated source was sent to a standard antenna about 2 m from the Trimble antenna. The same HP8565A analyzer used to acquire data on the RFI sources was configured as it had been for the experimental data. Trimble [Trimble,2001] supplied beam patterns for the antenna. In this way the signals were now calibrated at the level outside of the antenna.

There still is an uncertainty about the space loss and antenna beam pattern gain/loss for actual sources. The latter can be found for the signals located, but not unknown signals such as Source-2. Accordingly the data

were calibrated as a power level at the outside of the MBARI antenna.

COMPARISON TO A RFI SPECIFICATION

Figure 11 is a composite with one spectra, now calibrated to dBm outside the antenna and a specification for the RFI levels that aircraft GPS receivers used for critical phases of flight must meet. [RTCA, 1998]. The values measured from several other spectra taken at MBARI have also been plotted on this figure. Clearly these signals were above the narrow band limits by amounts from 3 to 24 dB.

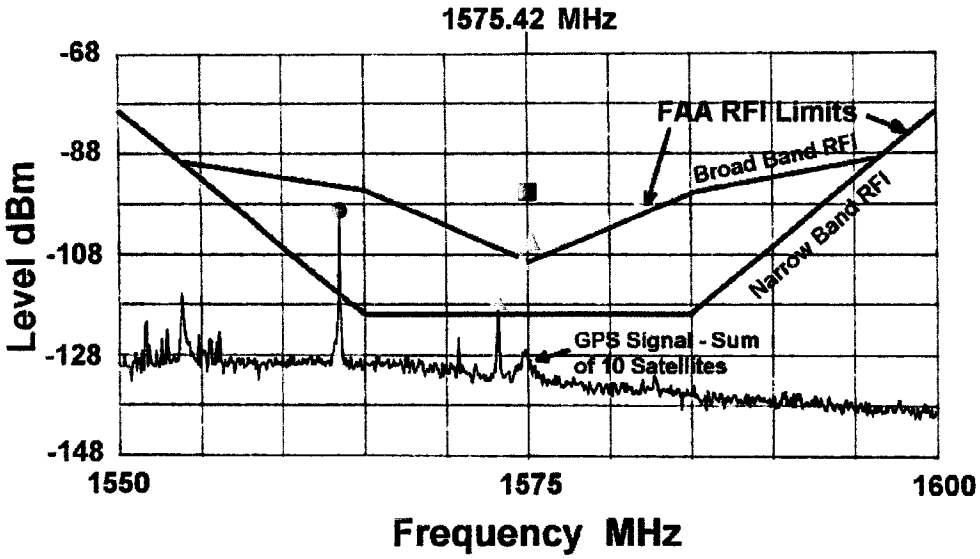

Moss Landing CA GPS RFI Spectrum July 10, 2001 With Previous RFI Measurements

RFI Source 1 Radio Shack TV Antenna

RFI Source 2 Unknown

RFI Source 3 Shakespeare TV Antenna

Figure 11

Source-1 had the highest level at -96 dBm. Its location is known to have been 325 m from the MBARI antenna. It was at an elevation angle of -2.5 degrees. While the beam pattern of Source-1 is unknown, if it were omni-directional, it would exceed this FAA specification at a range of 50 km or more. It is known to have caused marine GPS receivers to loose lock out to 3 km. The effective power of this source can only be bounded from the data available. It is at least a few milli-watts.

Source-2 varied in frequency and level. While on top of the L1 frequency it had a level of -106 dBm. Source-3 (Shakespeare Antenna) had a level at MBARI of -99 dBm. While it was about 12 MHz from the center of L1,

the variation in manufacture is likely to have produced units with emissions much nearer L1.

CONCLUSTIONS

In one small California harbor at least three emitters capable of jamming commercial GPS receivers were present. Two were located and removed by the authors. They were active UHF/VHF TV antennas, and appeared to have the same internal preamplifier. The FCC has located and removed the third.

The existence of the jamming was well known in the Moss Landing Harbor, and reported at least once to appropriate agencies. However the problem persisted until local engineers and scientist hunted down the worst offender. Clearly there was a system problem with reporting and removal of RFI sources. More education of harbor masters or some other change needs to be implemented to deal more quickly with this type of problem.

ACKNOWLEDGMENTS

The authors were assisted by many people in this effort. In particular Mr. Gary Thurmond, a retired MBARI engineer, provided technical advice and participated in the location of Source-1. Trimble Navigation provided a beam pattern for the specific antenna used on the MBARI roof.

REFERENCES

Clynch, James R., "Radio Interference with GPS at Moss Landing, CA Location and Initial Measurements", Memorandum, Department of Oceanography, Naval Postgraduate School, Monterey, CA, 29 May 2001.

Parker, Andrew A., Richard W. Adler, and Wilbur R. Vincent, "Parasitic Oscillation from an Active Television Antenna", Technical Memorandum, Signal Enhancement Laboratory Department of Electrical and Computer Engineering, Naval Postgraduate School, Monterey, CA, July 8, 2001.

RTCA, *RTCA DO-245*, "Minimum Aviation Performance Standards for GPS Local Area Augmentation System (LAAS)", September 28, 1998. [The same requirements are contained in the LAAS MOPS *RTCA DO-253* and WAAS MOPS, *RTCA DO-229*.]

NPS-EC-03-003

NAVAL POSTGRADUATE SCHOOL

Radio Interference from a Residential Solar-System Inverter

by

Wilbur R. Vincent
and
Richard W. Adler

October 2003

Approved for public release: distribution is unlimited

REPORT DOCUMENTATION PAGE

Form Approved
OMB No. 0704-0188

Public reporting burden for this collection of information is estimated to average 1 hour per response, including the time for reviewing instruction, searching existing data sources, gathering and maintaining the data needed, and completing and reviewing the collection of information. Send comments regarding this burden estimate or any other aspect of this collection of information, including suggestions for reducing this burden, to Washington headquarters Services, Directorate for Information Operations and Reports, 1215 Jefferson Davis Highway, Suite 1204, Arlington, VA 22202-4302, and to the Office of Management and Budget, Paperwork Reduction Project (0704-0188) Washington DC 20503.

1. AGENCY USE ONLY *(Leave blank)*	2. REPORT DATE October 2003	3. REPORT TYPE AND DATES COVERED Technical Report

4. TITLE AND SUBTITLE Radio Interference from a Residential Solar Inverter	5. FUNDING NUMBERS
6. AUTHOR(S) Vincent, Wilbur R. and Adler, Richard W.	
7. PERFORMING ORGANIZATION NAME(S) AND ADDRESS(ES) Signal Enhancement Laboratory Department of Electrical and Computer Engineering Naval Postgraduate School Monterey, CA 93943-5000	8. PERFORMING ORGANIZATION REPORT NUMBER NPS-EC-03-003
SPONSORING / MONITORING AGENCY NAME(S) AND ADDRESS(ES)	10. SPONSORING / MONITORING AGENCY REPORT NUMBER

11. SUPPLEMENTARY NOTES

The views expressed in this thesis are those of the authors and do not reflect the official policy or position of the Department of Defense, or other U.S. Government agency.

12a. DISTRIBUTION / AVAILABILITY STATEMENT	12b. DISTRIBUTION CODE
Approved for public release; distribution unlimited.	

13. **ABSTRACT *(maximum 200 words)*** *Harmful levels of radio interference at Amateur Radio Station K6GDI were traced to a residential solar system inverter. Examples of the level of the interference in the high-frequency band are presented. Examples of the magnitude of the EMI current flowing on the DC and AC conductors associated with the inverter over a wide range of frequencies are presented.*

14. SUBJECT TERMS Radio interference, radio noise	15. NUMBER OF PAGES 28
	16. PRICE CODE

17. SECURITY CLASSIFICATION OF REPORT	18. SECURITY CLASSIFICATION OF THIS PAGE	19. SECURITY CLASSIFI- CATION OF ABSTRACT	20. LIMITATION OF ABSTRACT
Unclassified	Unclassified	Unclassified	UL

CONTENTS

1. INTRODUCTION **1**

2. THE INTERFERENCE AT K6GDI **2**

3. SOURCE OF THE INTERFERENCE **7**

3.1 General Description **7**

3.2 Noise Current on DC Conductor **8**

3.3 Noise Current on AC Conductor **13**

4. DISCUSSION AND IMPLICATIONS **17**

5. CONCLUSIONS **20**

Appendix: INSTRUMENTATION **21**

LIST OF FIGURES

1.1 Satellite Photograph of Source and Victim Locations 1

2.1 Interference at K6GDI, 0- to 10-MHz 2

2.2 Interference at K6GDI, 3 to 5 MHz, Example 1 4

2.3 Interference at K6GDI, 3 to 5 MHz, Example 2 4

2.4 Interference at K6GDI, 6 to 8 MHz 5

2.5 Interference at K6GDI, 13.6 to 14.6 MHz 6

3.1.1 Photograph of Solar Inverter Unit 7

3.2.1 Noise Current, White DC Conductor, 0 to 2 MHz 8

3.2.2 Noise Current, White DC Conductor, 0 to 10 MHz 9

3.2.3 Noise Current, White DC Conductor, 10 to 20 MHz 10

3.2.4 Noise Current, White DC Conductor, 20 to 30 MHz 10

3.2.5 Noise Current, White DC Conductor, 30 to 80 MHz 11

3.2.6 Noise Current, White DC Conductor, 50 to 100 MHz 11

3.3.1 Noise Current, Black AC Conductor, 0 to 2 MHz 13

3.3.2 Noise Current, Black AC Conductor, 0 to 10 MHz 14

3.3.3 Noise Current, Black AC Conductor, 10 to 20 MHz 15

3.3.4 Noise Current, Black AC Conductor, 20 to 30 MHz 16

1. INTRODUCTION

Amateur radio station K6GDI reported the sudden appearance of severe radio interference in the 80- and 40-meter amateur radio bands and in the medium-wave broadcast band. The source of the interference was traced to the DC- to-AC power-conversion device associated with the installation of solar power at a nearby residence. This document provides technical information about the interference encountered at the K6GDI location, and it describes the conducted noise current carried by the DC to AC conductors associated with the solar inverter.

The owner of the inverter was very cooperative during the source-location work and during this later investigation of the properties of the noise current. He permitted access to the inverter for photographic purposes and for the measurements described in this document. In addition, he shut the system down for short periods of time to enable radio station K6GDI to participate in communications schedules and net-control activities. He also provided information about the sales organization that sold the converter and the manufacturer of converter.

Figure 1.1 shows a photograph of the locations of K6GDI and the residence with the solar system. This particular view was obtained from the GlobeXplorer satellite, and it provides a good view of the area. The distance between the solar inverter and K6GDI is about 0.21 miles.

Figure 1.1 **Satellite Photograph of Source and Victim Locations**

2. THE INTERFERENCE AT K6GDI

Since the primary interference encountered at K6GDI was in the 80 and 40-meter bands and the medium-wave broadcast band, the interference levels in these bands on nearby frequencies were examined at the input terminals of the receiver at K6GDI. The main HF antenna at the station was a 80-meter dipole elevated about 25-feet above ground. A coaxial cable ran from the center of the antenna to the receiver, a length of about 50 feet. This coaxial cable was extended to reach the instrumentation installed in a van located in the driveway of the K6GDI residence at 1172 Via del Sol, Salinas, CA 93907.

The instrumentation for the measurements is described in the appendix, and the key to a small table incorporated into each example of interference is provided in the appendix. This table identifies the primary instrumentation and measurement parameters used to obtain each item of data.

Figure 2.1 shows signals and interference received over the frequency range of 100 kHz up to 10 MHz. It is a typical amplitude-vs.-frequency view of signals and noise obtained from a scanning spectrum analyzer. Signals and interference below 100 kHz are not adequately shown in this example because of the limited low-frequency response of the current probe used for the measurements. In addition, a preamplifier was not used to avoid its saturation from the very high noise levels at the low end of the band.

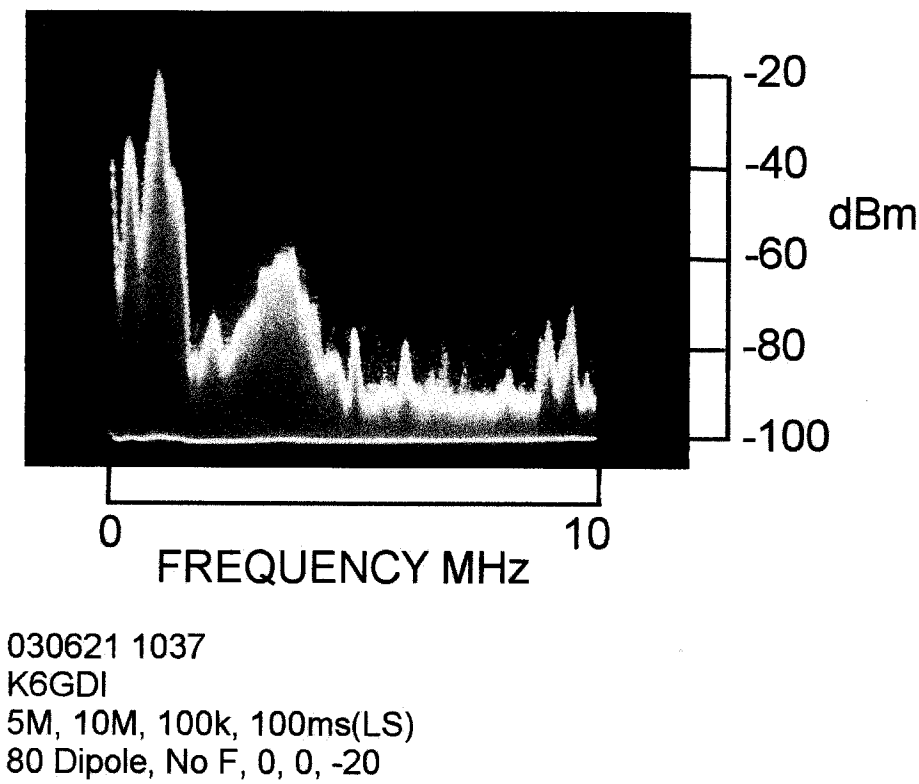

Figure 2.1 **Interference at K6GDI, 0- to 10-MHz**

The amplitude of the inverter interference at the K6GDI location over the 2- to 10-MHz band contains large-scale peaks and nulls across the frequency band. These peaks and nulls result from the radiation properties of the source, the added impact of the propagation path that contained hilly terrain and large trees, and the radiation properties of the receiving antenna. This resulted in a very strong peak in received interference that covered the entire 0.55- to 1.6-MHz medium-wave broadcast band. A second peak in interference covered the entire 80-meter amateur band (3.5 to 4.0 MHz). Lower levels of noise are shown at the 40-meter amateur band (7.0 to 7.3 MHz) along with a few high-level signals.

The data in Figure 2.1 and several subsequent examples was obtained using a rather wide measurement bandwidth of 100 kHz. This wide bandwidth was used to allow the examination of the gross spectral and temporal structure of the interference and to permit the full amplitude of impulsive components of received noise to be defined. The wide measurement bandwidth resulted in a high instrumentation-system noise floor compared to the noise floor provided by the much narrower bandwidth of a HF receiver, thus one must use the values of current on the examples of data with some caution. A procedure to scale the amplitude of the measured interference to the levels encountered by the narrower bandwidth of a typical HF receiver is provided in Section 4.

Figure 2.2 shows two views of interference from the inverter over the frequency range of 3 to 5 MHz. In this example a band-pass filter (with a pass band of 2 to 8 MHz) was used prior to the preamplifier. This filter attenuates interference below 2 MHz sufficiently that the instrumentation could examine low-level interference and signals at higher frequencies. The frequency range of this example includes the 80-meter amateur-radio band along with some margin on each end of the band.

A time-history presentation of the interference is shown in the lower view of Figure 2.2. This view shows some detail formed by the interaction between the wide-band and repetitive-impulsive structure of the interference and the scan process of the spectrum analyzer. Since the scan time is provided, the spacing between portions of the temporal structure can be determined. The upper view shows the spectral shape and amplitude of the same data at the input to the HF receiver at K6GDI. While there is a considerable variation in amplitude across the band, the interference is sufficiently strong to cover up all ambient signals.

Since the interference had a high impulsive content, the data in Figure 2.2 does not represent the actual signal-to-noise ratio encountered by a typical HF receiver operating at a much narrower bandwidth. Figure 2.3 shows the same frequency range but at a 3-kHz gaussian-shaped measurement bandwidth, a bandwidth much closer to the 2.8 kHz bandwidth of most HF receivers operating in the single-side-band mode. Less noise is passed by the narrower bandwidth, and a few discrete-frequency emissions appear above the non-flat noise in the upper view. Three of these emissions are believed to be strong amateur signals while the dense set of discrete-frequency emissions in the upper third portion of the band are from the inverter. The time-history view shows an on/off signal at 4 MHz. This emission was also traced to the solar converter.

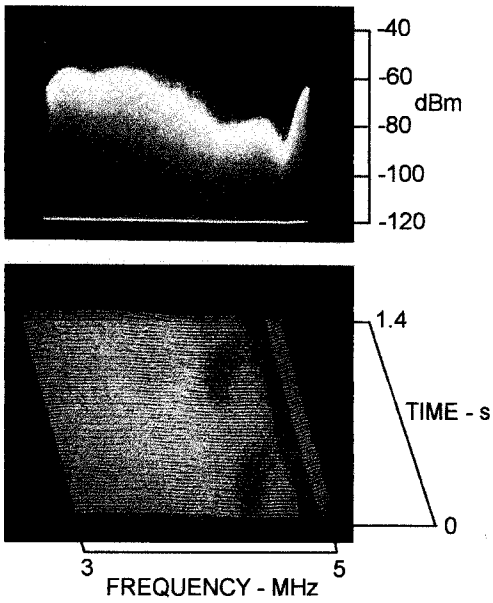

030621 1052
K6GDI
4M, 2M, 100k, 20ms
80 Dipole, F(2-8), +20, 0, -20

Figure 2.2 **Interference at K6GDI, 3 to 5 MHz, Example 1**

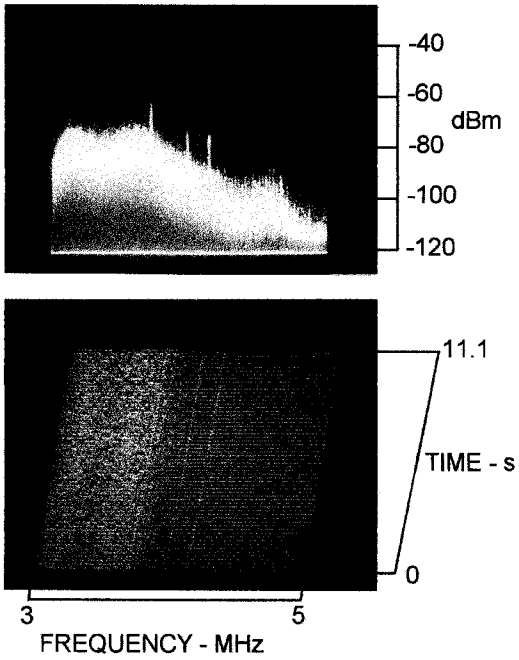

0330621 1059
K6GDI
4M, 2M, 3k, 100ms
80 Dipole, F(2-30), +20, 0, -20

Figure 2.3 **Interference at K6GDI, 3 to 5 MHz, Example 2**

Figure 2.4 shows the spectral and temporal structure of the solar inverter interference from 6 to 8 MHz. This range contains the 40-meter amateur band. The time history view shows considerable temporal structure from the impulsive content of the interference. Two sets of distinctive slanting lines in the upper third of the frequency range indicate that two distinct processes exist within the source with slightly different times between noise pulses. The spacing between the two sets is nearly the same (about 22.73 ms), but the differences in slope between the two indicate that a small difference exists in their periods.

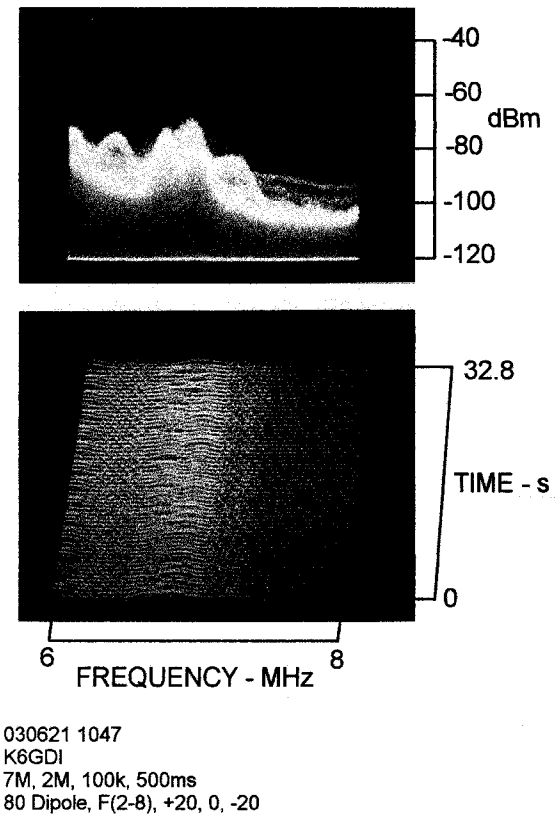

Figure 2.4 **Interference at K6GDI, 6 to 8 MHz**

Additional slanting lines at still a different slope exist below 6.7 MHz and immediately above 7 MHz. The pulses are wider for this set and the period between pulses is less. Thus three different and distinct timing functions exist in the interference received at K6GDI. While the periods of the three sets of slanting lines cannot be precisely determined from scaling the time-history view, approximate values can be obtained. None of the sets appear to be related to the 60-Hz line frequency of the commercial electric power available at the residence.

Additional measurements in and around the 20-meter amateur band were made to obtain some information about the upper frequency limit of the interference. These measurements were made from the 80-meter dipole since it was the most assessable antenna.

Figure 2.5 shows two views of the interference over the 13.6- to 14.6-MHz frequency range. The upper view shows that the amplitude of the interference varied considerably across the frequency range. A few strong signals exceed the interference level, but interference covered up all low- and modest-level signals. The noise floor of the measurement system for the 10-kHz bandwidth of the example is about –124 dBm, but the interference level was sufficiently high that the inverter noise is well above the measurement-system noise floor. It is expected that the inverter noise levels would be even higher if a more appropriate 20-meter antenna had been used.

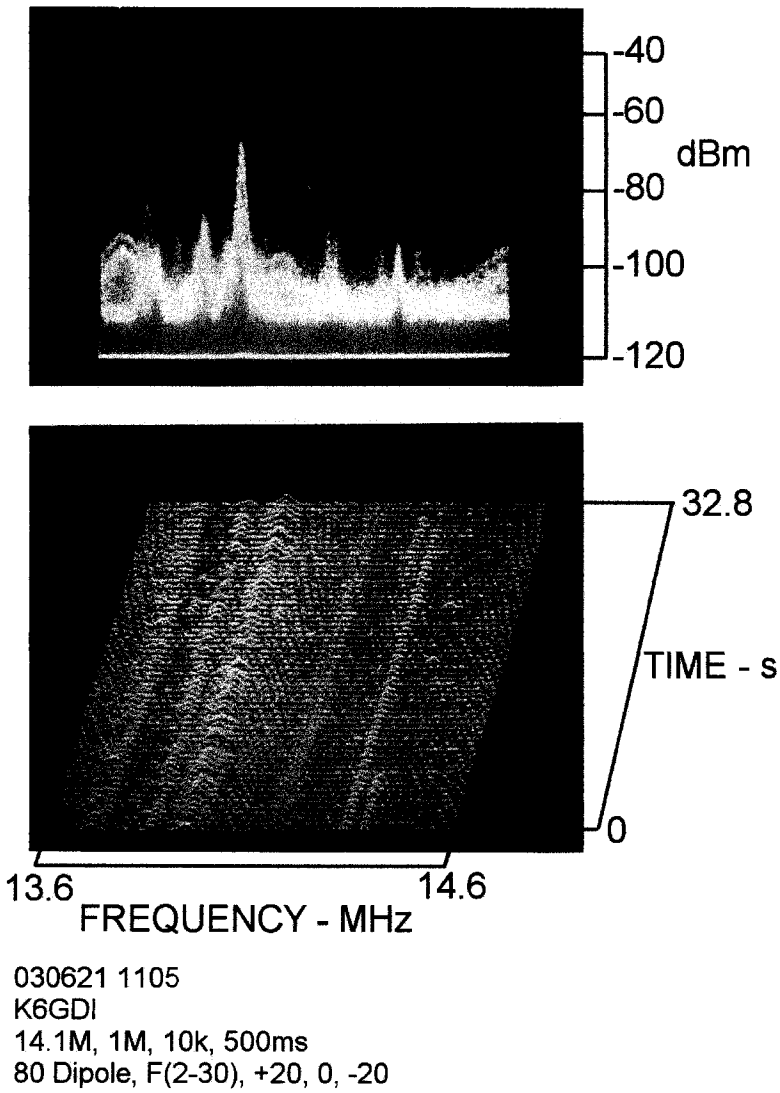

Figure 2.5 **Interference at K6GDI, 13.6 to 14.6 MHz**

The time-history view shows that the noise is highly impulsive. Furthermore, the curved lines of the pulse pattern shows that the impulse rate of the source changed slightly during the measurement period.

THE SOURCE OF THE INTERFERENCE

3.1 General Description

The instrumentation was moved to the source location on completion of the measurement and documentation of the interference at the K6GDI location. The source had been previously tracked down and identified by K6GDI. Arrangements had been made to park the instrumentation van in the driveway of the source residence at 1177 Via del Sol, Salinas, CA to measure noise current on the conductors associated with the solar inverter unit.

Figure 3-1 is a photograph of the inverter unit. It is located on a wall of a closet at the rear of the garage. The closet contained the inverter, a water heater and other small devices associated with the residence. The lower cover of the inverter enclosure was removed to expose the white and red DC conductors running from the inverter to solar cells on the roof and the AC conductors running from the inverter to the house wiring.

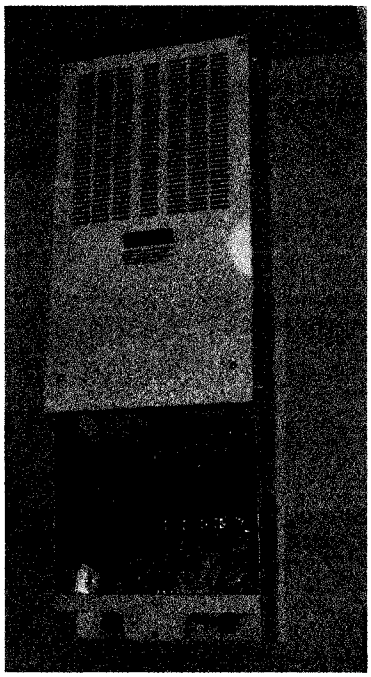

Figure 3.1.1 **Photograph of Solar Inverter Unit**

A label on the right side of the unit identified the manufacturer of the Inverter.[1] It was purchased through a dealer.[2] Of interest is that the usual label indicating the device meets either the FCC Class A or Class B noise requirements for electronic devices marketed to the public was not found on the inverter.

---

[1] Photovoltaic Power Inverter, Model ST2500, manufactured by Trace Engineering of Arlington WA, 98223. The telephone number (380) 435-8826 was also on the label. Further investigation indicates Trace Engineering has been purchased by xantrex Technology Inc, of Vancouver, British Columbia although the Trace facility appears to now be operating as a unit of xantrex.

[2] Solatron Technologies, Inc., 15663 Village Drive, Victorville, CA 92394, Telephone (760) 955-3416.

A Fischer Custom Communications Model F-70 Current Probe was used to measure broad-band noise current flowing in the DC and AC conductors associated with the solar inverter. This particular probe is flat in frequency response from 100 kHz up to 100 MHz. Harmonic and other components of noise at lower frequencies were not examined with a low-frequency probe due to the lack of time.

3.2 Noise Current on the White DC Conductor

Figure 3.2.1 shows noise current flowing on the white DC conductor over the frequency range of 100 kHz up to 2 MHz. This conductor ran from the inverter unit to the rooftop solar cells, a distance of more than 50 feet. Only an approximation of the length of the DC conductors was possible since they were installed behind walls during the construction of the residence. A very strong spectral peak in the noise current is shown near 100 kHz with another broad peak slightly above 1 MHz (the middle of the medium-wave broadcast band). Numerous close-spaced spectral components are shown throughout the frequency range. The time-history view shows the spectral and temporal properties were stable over the measurement period.

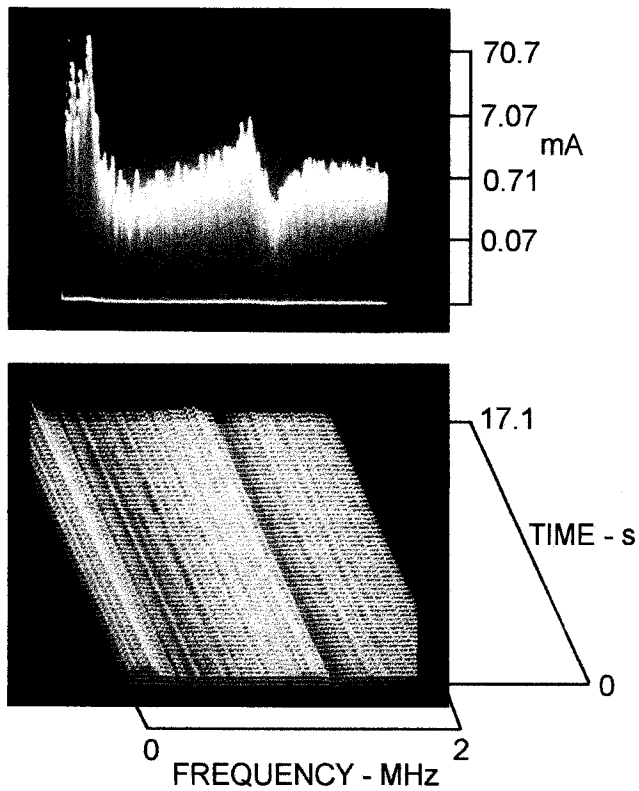

030621 1253
1177 Via del Sol, White DC
1M, 2M, 10k, 200ms
F-70, 0, -10, -10

Figure 3.2.1 **Noise Current, White DC Conductor, 0 to 2 MHz**

The total noise power at the low frequencies was sufficient to exceed the dynamic range of the measurement system when it was operated at maximum sensitivity. This made it necessary to use a high-pass or a band-pass filter between the current probe and the measurement system to examine lower-level inverter noise at frequencies above 2 MHz. This filter was a high-power unit designed to avoid saturation of its components from the high power levels encountered during the measurement.

Figure 3.2.2 shows the noise current level on the White DC conductor over the frequency band of 2 to 10 MHz. A peak in the spectral content of the noise current is shown at about 2.5 MHz followed by a sharp dip and then decreasing values to the upper limit of the measurement of 10 MHz.

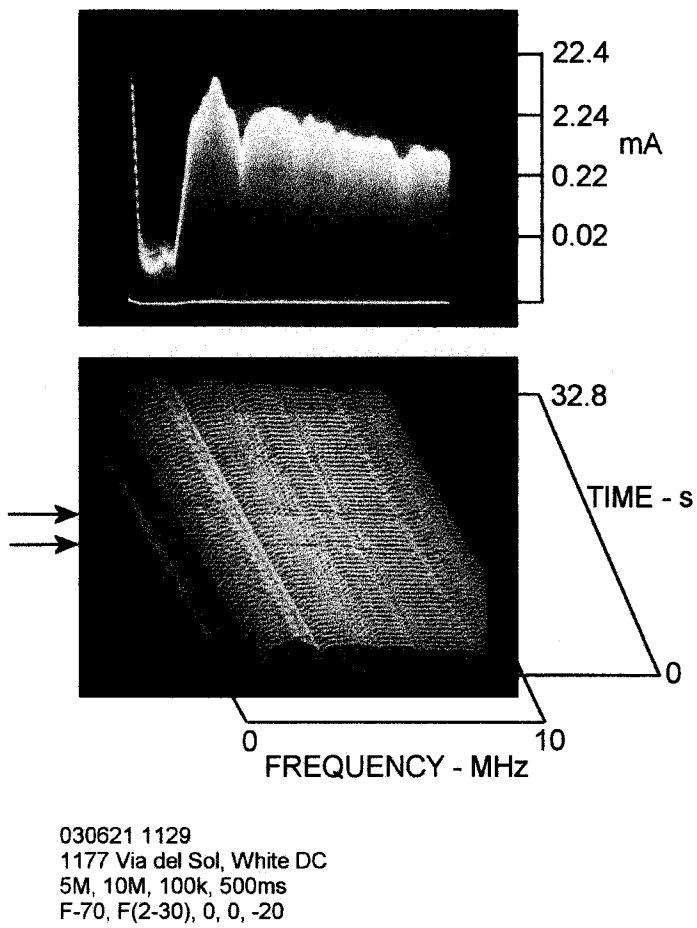

Figure 3.2.2 **Noise Current, White DC Conductor, 0 to 10 MHz**

Two arrows are shown on the left side of the time-history view of Figure 3.2.2. These arrows point to two small changes in the spectral structure of the noise current observed during the measurement time.

Additional measurements were made at higher frequencies in 10- and 50-MHz increments of frequency, and the results are shown in Figures 3.2.3 through 3.2.6.

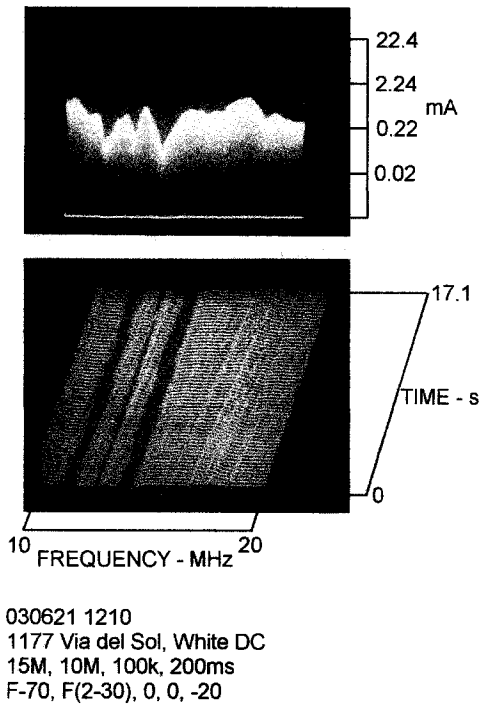

Figure 3.2.3 **Noise Current, White DC Conductor, 10 to 20 MHz**

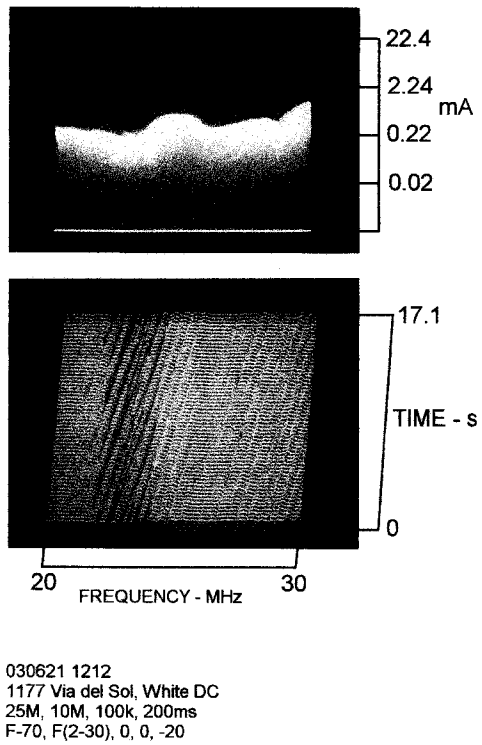

Figure 3.2.4 **Noise Current, White DC Conductor, 20 to 30 MHz**

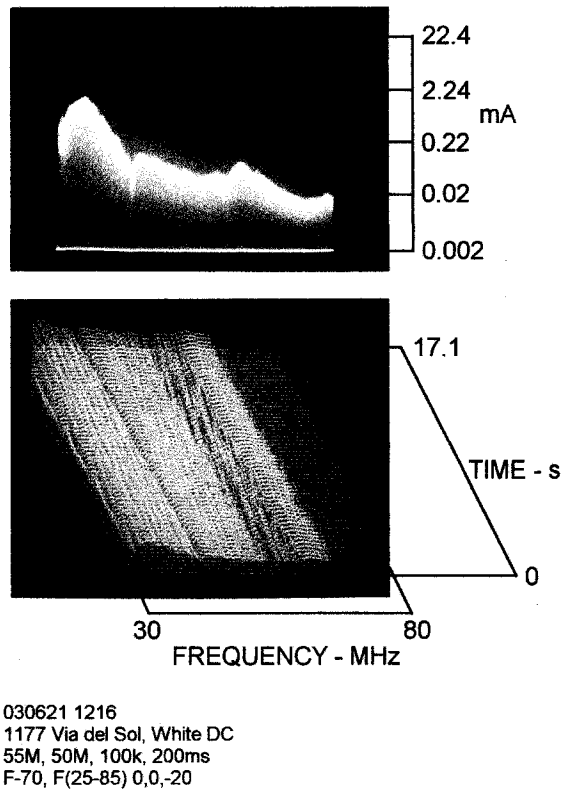

Figure 3.2.5 **Noise Current, White DC Conductor, 30 to 40 MHz**

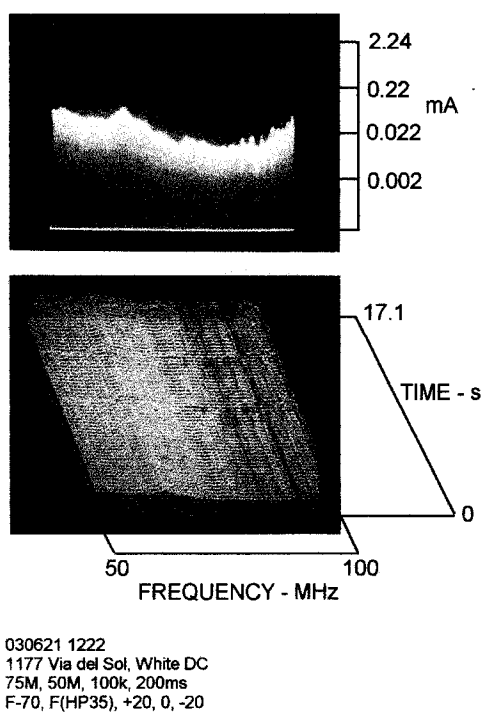

Figure 3.2.6 **Noise Current, White DC Conductor, 50 to 100 MHz**

Figure 3.2.3 shows significant peaks and nulls in the amplitude of the noise current over the 10- to 20-MHz frequency range. This is probably because the length of the White DC conductor and its inductive coupling to other nearby conductors is sufficient to support resonance conditions similar to those found with antennas and transmission lines. The time-history view shows the slanting lines typical of a high impulsive content of the noise current.

Figure 3.2.4 shows broad variations in the amplitude of the noise current over the 20- to 30-MHz frequency range. In addition, the amplitude increased with frequency by a factor of about 5.

Figure 3.2.5 shows the noise current generally decreased with increasing frequency over the frequency range of 30 to 80 MHz.

Figure 3.2.6 shows the noise current over the frequency range of 50 to 100 MHz. The instrumentation preamplifier was used over this frequency range, and the amplitude scale takes into account the 20-dB gain of the preamplifier. While the amplitude of the noise current decreased over the 50- to 85-MHz range, it increased in amplitude at frequencies above 85 MHz. Since 100 MHz was the upper limit of the spectrum analyzer RF head used for the measurement, the noise current was not measured at higher frequencies. Also, it was not anticipated that measurements would be useful at frequencies above 100 MHz during the measurement planing sessions. This assumption was incorrect since the noise current levels on both the DC and AC conductors were sufficiently high to degrade the reception of VHF signals at locations near the inverter.

The time-history view of Figure 3.2.6 shows two brief changes in the spectral properties of the noise current. This implies that a load changed or an inverter control function occurred during the measurement.

3.3 Noise Current on the Black AC Conductor

At the completion of the measurement of noise current on the DC conductors running from the inverter to the solar cells, noise current was examined on the AC conductors running from the inverter to the house wiring. Figure 3.3.1 shows noise current over the frequency range of 100 kHz to 2 MHz. Current at lower frequencies was not examined (including harmonics and other spectral components generated by the inverter) due to the lack of time to complete a comprehensive set of measurements. The very high peak in current at the low end of the frequency scale suggests that high levels of harmonic current are present, and they should be measured to obtain a complete understanding of the noise generated by the inverter throughout the radio spectrum. The noise current was quite low from about 200 kHz up to about 1 MHz. It then reached a peak of about 2 mA near 1.2 MHz followed by a series of peaks and nulls.

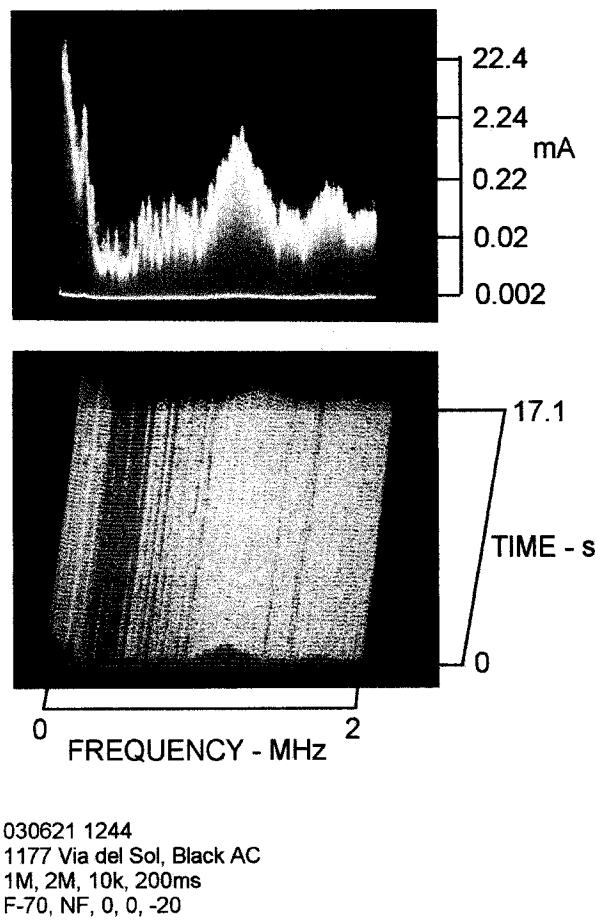

Figure 3.3.1 **Noise Current, Black AC Conductor, 0 to 2 MHz**

The spectral shape of the AC noise current over the frequency range of 100 kHz to 2 MHz is crudely similar to that for the DC noise current in Figure 3.2.1. While the amplitude of the peak current on the AC conductor at 1.2 MHz appears to be about 10-dB lower than on the DC conductor, this series of measurements was made at a measurement bandwidth of 10 kHz. Applying the bandwidth conversion factor of 19 dB to the data

(see Figure 4.1) indicates that noise current on the AC conductors over this frequency range is about the same or slightly higher in amplitude than on the DC conductors. No significant change in the spectral or temporal structure of the current was found over the measurement time.

Figure 3.3.2 shows noise current on the AC conductor over the frequency range of 0 to 10 MHz. The lack of current below 2 MHz is caused by the use of a filter prior to the preamplifier. The filter was added to allow the instrumentation to examine low levels of noise current at the higher frequencies without encountering saturation from lower-frequency spectral components. The shape of the spectrum of the current from 2 MHz to 10 MHz is somewhat different than for the similar example for the DC current (i.e. see Figure 3.3.2), but some characteristics are similar. When the bandwidth conversion is applied to the data, the noise on the AC conductors is higher than on the DC conductors.

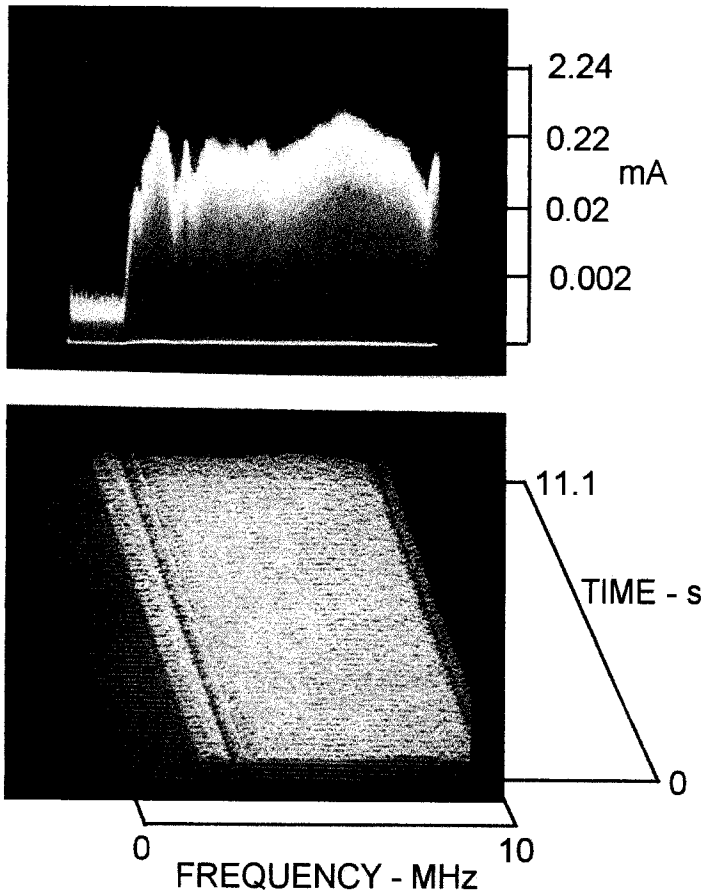

030621 1302
1177 Via del Sol, Black AC
5M, 10M, 10k, 100ms
F-70, F(2-30), +20, 0, -20

Figure 3.3.2 **Noise Current, Black AC Conductor, 0 to 10 MHz**

Figure 3.3.3 shows noise current on the AC conductor over the frequency range of 10 to 20 MHz. Several peaks and nulls are shown that are different from current on the DC conductor (see Figure 3.2.3 for a comparison). The amplitude of the current is about the same as for the DC conductor when the bandwidth-scaling factor is taken into account.

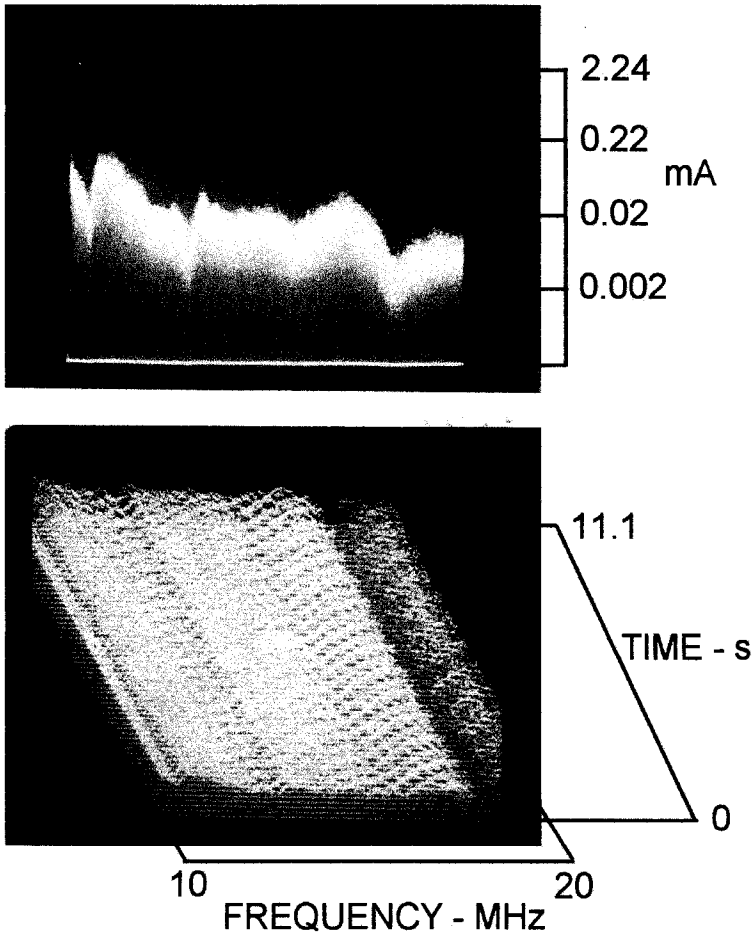

030621 1258
1177 Via del Sol, Black AC
15M, 10M, 10k, 100ms
F-70, F(2-30), +20, 0, -20

Figure 3.3.3 **Noise Current, Black AC Conductor, 10 to 20 MHz**

Figure 3.3.4 shows the level of noise current on the black AC conductor over the frequency range of 20 to 30 MHz. In this case the peaks and nulls in current shown in the upper view are roughly similar to those on the DC conductor (i.e. see Figure 3.2.4). A broad null in current occurs near 22.5 MHz and a peak occurs near 25 MHz in both examples. When the bandwidth compensation factor is considered, the current amplitude is about the same at that on the DC conductor. The slanting lines in the time-history view indicate that the noise has a high impulsive content.

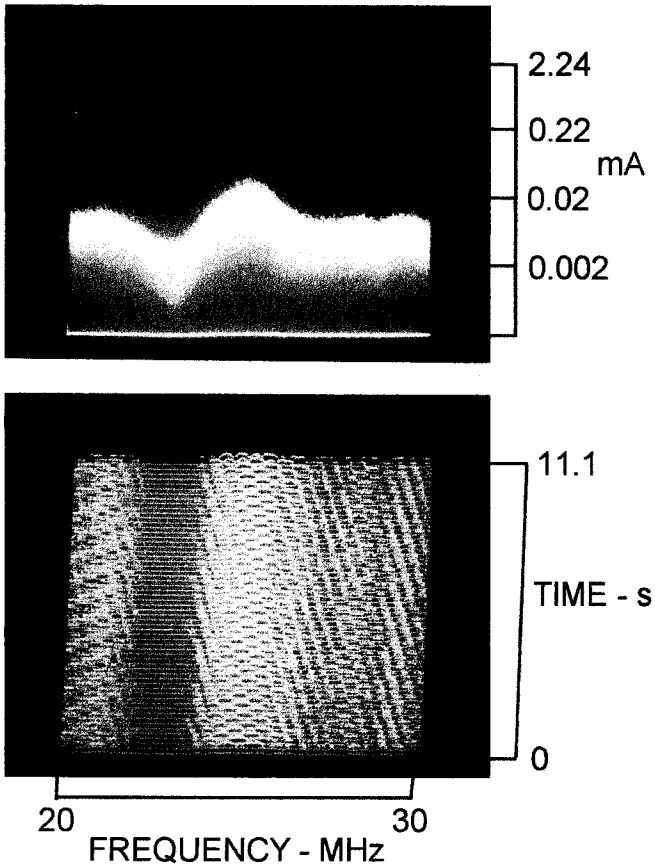

030621 1253
1177 Via del Sol, Black AC
25M, 10M, 10k, 100ms
F-70, F(2-30), +20, 0, -20

Figure 3.3.4 **Noise Current, Black AC Conductor, 20 to 30 MHz**

4. DISCUSSION AND IMPLICATIONS

Amateur radio station K6GDI is located in a rural area containing low-density housing that is generally free of sources of man-made radio noise. It is considered to be an ideal location for amateur radio purposes and other signal-reception tasks. For example, K6GDI is often requested to monitor HF frequencies for scientific purposes, and this has significantly aided the staff of the Naval Postgraduate School in the conduct of HF propagation studies.

The levels of interference at K6GDI from the solar inverter clearly made communication impossible in both the 80- and 40-meter amateur radio bands. Also, reception in the 20-meter amateur band was sufficiently degraded that only very strong signals could be received, a condition that prevented the normal use of that band. In addition, the interference prevented the reception of most medium-wave broadcast-band signals, especially the popular AM stations located in Monterey and San Francisco. Furthermore, interference from the solar inverter interfered with the reception of all other LF, MF, and HF signals up to at least 20 MHz. Reception at higher HF-frequencies is believed to also be degraded but interference in that portion of the HF band was not examined due to the limited time available to document the full extent of the interference.

Measurements at the source verified that the solar inverter was the source of the interference at K6GDI. In addition, on/off tests had previously been conducted with positive results. The documentation of the spectral and temporal properties of inverter-generated conducted noise current on the DC and AC conductors indicates the source clearly exceeds reasonable levels for use in a residential area or any area near a housing area. The DC and AC conductors of the residence were effective antennas that radiated inverter-generated radio noise over a widespread area surrounding the source. It is suspected the noise was also conducted onto the overhead distribution lines serving the solar-equipped house, and radiation from the distribution lines probably also contributed to the noise encountered at the K6GDI location, but this could not be investigated during the short time available for the measurements.

Many of the measurements were made at a Gaussian-shaped bandwidth of 100 kHz. This was done to best portray the spectral and temporal properties of the interference at the K6GDI location and conducted current at the solar-inverter location. The amplitude of time-stable Gaussian noise can be scaled by conventional rules to other bandwidths. Discrete-frequency emissions are not a function of bandwidth and are not affected by the measurement bandwidth. However, the solar-inverter interference is highly impulsive and its amplitude is a function of bandwidth. Since a theoretical means to establish a relationship between impulsive noise level and bandwidth is not feasible, Hodge[3] examined the amplitude/bandwidth-scaling problem at a number of HF sites. He made extensive measurements of impulsive noise at multiple bandwidths and developed an empirical curve for bandwidth scaling. His curve is reproduced below to permit

[3] James Hodge, A comparison between Power-Line Noise Level Field Measurements and Man0Made Noise Prediction Curves in the High Frequency Band, MS Thesis, Naval Postgraduate School, Monterey, CA, December 1995

scaling the inverter noise to any reasonable bandwidth of interest. The curve for scaling Gaussian noise is also included for reference purposes.

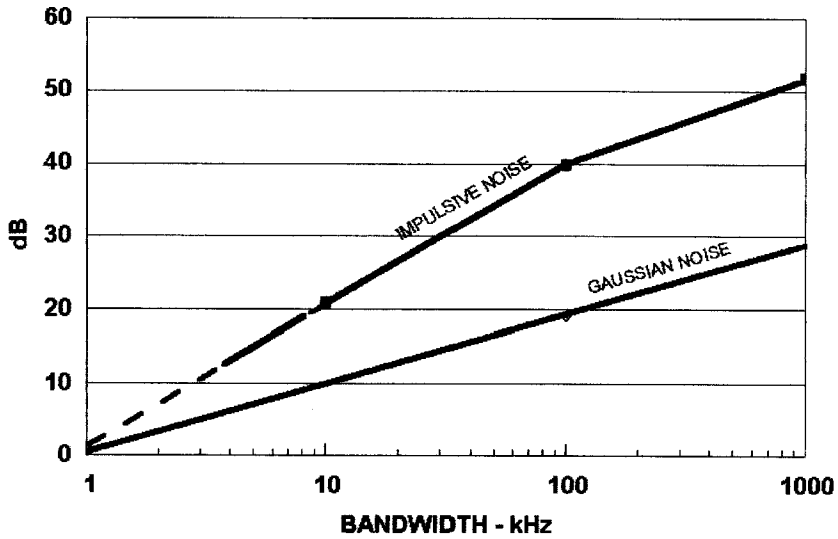

Figure 4.1 **Impulsive and Gaussian Noise Scaling Curves**

The measured data indicate the noise current generated by the solar inverter must be reduced by 70 to 80 dB to completely avoid harmful interference at the K6GDI location. This amount of reduction is feasible by the proper design of the inverter enclosure and the use of filters on each conductor penetrating the enclosure. Unusual gaskets on seals are not needed on the enclosure, but the careful physical and electrical layout of filters for each conductor is essential. Shielding the DC and the AC conductors will not correct the problem since the far end of these conductors cannot be terminated within a shielded enclosure.

Since the driving impedance of the DC and AC conductors was not measured, it was not possible to provide an accurate estimate the noise power produced by the inverter. This measurement would have required a number of additional actions such as:

(1) the shut down of the inverter,
(2) the removal of the both the AC and DC conductors from the inverter,
(3) the disconnection of the solar cells from the Red and White Conductors and their replacement by an equivalent electrical circuit, and
(4) the removal of commercial electrical power from the residence.

These added tasks were beyond the scope of this effort. While of scientific interest, this additional effort was not required to identify and document the source of the radio interference to K6GDI.

Crude estimates of the noise power delivered to the instrumentation were made to verify that precautions were necessary to avoid overloading the instrumentation. Since the output impedance of the Model F-70 Current Probe was 50 Ohms and the impedance of all other RF portions of the instrumentation was at 50 Ohms, it was possible to obtain an estimate of the noise power of the major spectral peaks. Figure 3.2 shows the noise

current at 1 MHz to be about 70 mA, an unusually high value for noise current on a conductor associated with an electronic device located in a residence. From this we can estimate the noise power at the input to the instrumentation.

$$P = I^2 \times R$$

Where:

P is the power at the input to the instrumentation
I is the measured current
R is the 50-Ohm resistive impedance of the RF path

From this we find the power applied to the instrumentation at 1 MHz to be about 0.25 Watts in a narrow bandwidth centered at 1 MHz. The total noise power over the entire spectral width of the noise would be even higher. This is a very high power level to apply to standard RF components, and it shows that instrumentation must be selected that will not overload or saturate. For example, the filters used in these measurements were designed to handle a total input power of 1 Watt.

Since it is expected that the driving impedance of the current loop created by the White DC wire, the solar cells, and the Red DC wire will be much higher than 50 Ohms, the RF power flowing on those conductors will be much larger than that delivered to the instrumentation. For example, a value of 1000 to 5000 Ohms might be a reasonable value for the impedance of this loop at 1 MHz. This would result in a power level of 5 to 25 watts at the 1-MHz peak of inverter noise, a very high level of RF power. This narrow-band value does not provide an estimate of the even higher total broadband noise power generated by the solar inverter and radiated by its associated conductors.

One further aspect of noise generated by the solar inverter is of interest. The inverter did not have the Federal Communications Commission label indicating it meets the noise levels required for a Class A or Class B device[4]. Class B devices marketed for residential use must meet more stringent requirements than Class A devices which are intended for industrial use.

The measurement team appreciated the complete cooperation and the assistance of the owner of the solar inverter during the effort described in this document. He innocently purchased the unit through a standard dealer who was selling the standard product of a manufacturer. Information was not provided by the dealer or the manufacturer that this device might generate harmful levels of radio noise or that it did, or did not, meet Federal Communications Commission requirements for electronic devices.

[4] Look up the proper reference

5. CONCLUSIONS

Two primary conclusions were reached from this effort.

1. The solar inverter located at 1177 Via del Sol, Salinas CA is a major source of harmful levels of radio noise to a licensed radio station and operator. It also adversely affected medium-wave broadcast-band reception at K6GDI and at other nearby residences.
2. The solar inverter appears to not meet the Class B requirement of the FCC for electronic devices marketed to the public for use in residential areas, and it is doubtful the device will meet the FCC Class A requirement for use in industrial areas. Since the device did not contain the usual label required by the FCC for electronic devices, it appears not have been tested for either application.

In addition to the primary conclusions above, the team that investigated this severe radio-interference problem expresses our thanks to the occupants of the residence containing the solar inverter and to K6GDI. Their complete cooperation allowed the problem to be investigated, understood, and documented.

The measurement team is dismayed to encounter an electronic product sold to the general public that is clearly a major source of harmful radio noise. Several additional cases of such interference have recently come to the attention of the measurement team, and more are expected in future times as the numbers of residential and business solar power installations grows. Straightforward engineering techniques can correct this problem without altering the performance of an inverter.

Appendix

INSTRUMENTATION

INSTRUMENTATION

A photograph of the instrumentation used for the measurements at K6GDI is shown in Figure 1, and a block diagram is shown in Figure 2. This instrumentation was installed in a small van equipped with a diesel power generator for portable and mobile operation.

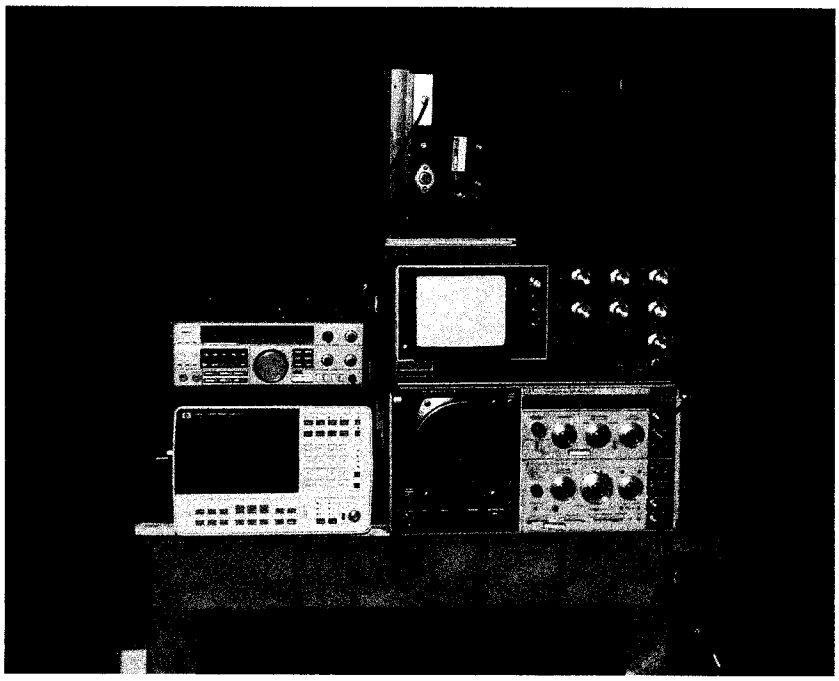

Figure 1 **Photograph of Instrumentation**

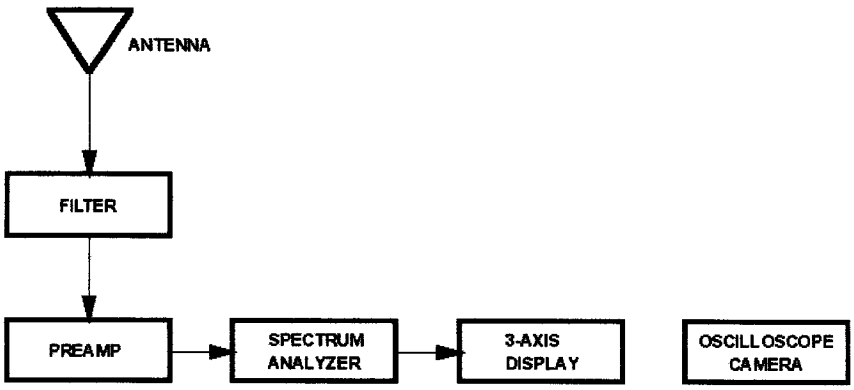

Figure 2 Block Diagram of Instrumentation

The primary components of the instrumentation are described in the sequence shown in the block diagram. In this case, antennas available at the K6GDI location were used, thus the measurements represent the signal-to-noise encountered at the input to the K6DGI receiver. For measurements at the noise source, the antenna was replaced with a Fisher Model F-70 Current Probe.

A set of low-pass and band-pass filters was provided to allow the examination of low-level signals at frequencies higher than the dominant spectral components generated by the inverter. All filters were designed to cope with high-level signal and noise power levels without incurring saturation of their components.

A high dynamic range HF preamplifier with a frequency range of 100 kHz to 100 MHz was provided. Its gain of 20 dB was sufficient to overcome the relatively poor noise figure of the spectrum analyzer and provide a signal-detection capability about equal to that of a standard HF receiver. The noise figure of this amplifier was 12 dB, again about equal to most standard HF receivers. While this preamplifier is significantly more robust that the amplifiers found in most receiving systems, it is still subject to overloading under some severe high-level signal and noise conditions. For this reason the filters described above were available to eliminate unusually high-level signals and noise from reaching the preamplifier. For some measurements where unusually high signal and noise conditions were encountered, the preamplifier was removed.

A HP Series 141 Spectrum Analyzer Main Frame was used. A HP Model 8553L Spectrum Analyzer RF Head was provided to allow signal and noise measurements over the frequency range of 10 kHz to 110 MHz. A HP Model 8552A Spectrum Analyzer IF Head was provided to control the operation of the analyzer. The blanking times of this particular head were carefully measured to allow the calibration of the time-axis of the time-history display used to observe and record data.

A ELF Model 7200B 3-Axis display was provided to portray a wide variety of signal and noise conditions. The time-history presentation of this unit is especially valuable in providing an operator with a real-time view of the spectral and temporal details of signals and noise.

Since the Model 7200B display employs time in the presentation of data, it was necessary to accurately measure the blanking time of the spectrum analyzer at all scan-time settings used for the collection of data. Thus the time-axis duration of the Model 7200B display (T_t) is determined by the operating parameters of the spectrum analyzer. It is calculated for each scan-time setting of the analyzer by the following formula:

$$T_t = (T_s + T_b)\, 60$$

where:

T_s is the total scan time of the analyzer

T_b is the blanking time of the analyzer for each setting of the scan time control.

Table 1A provides the scan-time information as well as the resulting time-axis duration of the Model 7200B display when the spectrum analyzer is operated in its normal free-running mode.

Table 1A
Blanking Time Information, Free-Running Mode

Total Scan Time ms	Measured Scan Time ms	Measured Dead Time ms	7200B Time Axis s
2	1.8	0.38	0.13
5	5	0.38	0.32
10	9.6	2.7	0.74
20	19.2	4.7	1.43
50	50	4.7	3.28
100	100	84	11.1
200	200	84	17.1
500	510	82	35.5
1000	1000	81	64.7
2000	2000	82	124.9
5000	5200	80	316.8

Table 1B provides the scan-time information as well as the resulting time-axis duration of the Model 7200B display when the spectrum analyzer is operated in its line-sync mode.

Table 1B
Blanking Time information, Line Sync Mode

Total Scan Time ms	Measured Scan Time ms	Measured Dead Time ms	7200B Time Axis s
2	2	14.6	1.0
5	5	11.7	1.0
10	10	7	1.0
20	20	13	2.0
50	50	32	4.9
100	100	100	12.0
200	200	82	16.9
500	510	70	34.8
1000	1000	82	64.9
2000	2000	92	125.5
5000	5200	96	317.8

The combination of the real-time spectrum analyzer and time-history presentations allows an operator to rapidly adjust each instrument to best view and document any desired signal or noise condition. The low blanking time of the spectrum analyzer used, compared to newer models, and the visual adjustments of the 3-axis display are especially useful in viewing and documenting signal and noise conditions. They provide a means to show the coarse-scale properties of signals and noise in any

portion of the HF or VHF/UHF bands or to show the fine-scale properties of any desired signal or noise. This type of information allows the instrumentation operators to immediately identify the primary properties of signals and noise, and it also provides a rapid means to identify the type of source involved in the generation of man-made noise. The time-history presentation is especially useful in presenting and understanding time-varying cases of man-made noise.

A Tektronix Model C5-C Oscilloscope Camera is used to photograph any desired view of signals and noise appearing on the Model 7200B display.

Photographs of data are scanned into computer files in the field with a Cannon Model 655U Scanner connected to a Compaq Armada E-500 Laptop Computer. Paint Shop Pro, Version 5, was used to add frequency, time, and amplitude scales to the data. The resulting digital files of each item of data are then inserted into the text of a field report.

Additional instrumentation was available to examine spectral components generated by the inverter over the frequency range of 10 Hz to 100 kHz. This instrumentation consisted of a Tektronix Model C5/P6021 Current Probe, a WRV Model 101 Line Amplifier, and a HP Model 3561A Spectrum Analyzer. While this instrumentation was available, there was not sufficient time to employ it to examine harmonics and other low-frequency components.

A small table accompanies each item of data in this document. This table provides key information about each measurement and the instrumentation setting used to obtain each item of data. The parameters of the table are:

Table 2
Measurement and Instrumentation Parameters

Line 1	Date in yymmdd format, Local Time
Line 2	Location, Source Identification Information
Line 3	Center Frequency, Frequency Width, IF Width, Scan Time
Line 4	Source, Filter, Preamp Gain, RF Attenuation, IF Gain
Line 5	Additional Information as Required